Mon. Not. R. astr. Soc. (1988) **231,** 795–821

Sonic instabilities in supersonic shear flows

W. Glatzel *Max-Planck-Institut für Astrophysik, Karl-Schwarzschild-Straße 1, D-8046 Garching bei München, Federal Republic of Germany*

Accepted 1987 October 14. Received 1987 September 24; in original form 1987 July 27

Summary. Using analytical methods the stability of a linear supersonic shear layer is re-examined. Two mechanisms working both for Kelvin–Helmholtz-type modes and sonic modes are responsible for instabilities caused by the shear: resonant interaction between modes and energy loss due to acoustic radiation of modes having negative energy. Which of these mechanisms is dominant sensitively depends on the density contrast between the shear layer and the surrounding medium. A close relation to the instability of accretion tori discovered by Papaloizou & Pringle is found.

1 Introduction

The stability of a shear layer is a fundamental problem in fluid dynamics and has been studied by many authors since the first investigations by Kelvin and Helmholtz in the last century. In this paper we shall concentrate on the stability properties of a simple linear shear layer having a supersonic velocity difference across the layer, a case which has previously been considered by Ray (1982) and Choudhury & Lovelace (1984).

Apart from applications to laboratory flows (*cf.* Blumen, Drazin & Billings 1975) there is a variety of astrophysical situations in which the stability of supersonic shear layers probably plays an important role, e.g. the boundaries between different sectors of the solar wind or the boundaries of galactic and extragalactic jets (*cf.* Choudhury & Lovelace 1984). In particular, the wiggles observed in radio jets may be due to instabilities occurring at the boundaries of the flow (Hardee 1979). Except the investigation by Ferrari, Massaglia & Trussoni (1982) the stability of the boundary between two flows having a supersonic velocity difference has been studied either in the vortex sheet approximation or for smooth velocity profiles with equal sound velocity inside and outside the shear layer (Blumen *et al.* 1975; Ray 1982; Ferrari & Trussoni 1983; Choudhury & Lovelace 1984). It has been found that the modal structure of the vortex sheet is markedly different from that of smooth velocity profiles (Choudhury & Lovelace 1984) but the modal structure of different smooth velocity profiles (including the linear profile) is at least qualitatively similar (Ray 1982). According to Ferrari *et al.* (1982) different densities inside and outside the flow in connection with a shear layer lead to a decrease of growth rates of Kelvin–Helmholtz type instabilities and for high-density contrast possibly to stability.

Here we shall reconsider the stability properties of the linear shear layer using various kinds of boundary conditions for the perturbed quantities. In particular, these boundary conditions will be chosen to allow for a different density of the shear layer and the surrounding medium. A second question we shall address in this paper is whether there is a relation between the instability of accretion tori found by Papaloizou & Pringle (1984) and later discussed by several authors (*cf.* Blaes 1985; Drury 1985; Goldreich & Narayan 1985; Goldreich, Goodman & Narayan 1986; Hanawa 1986; Papaloizou & Pringle 1985, 1987 and references therein) and the instability of a simple linear shear layer as investigated here.

2 Basic equations

We consider the linear stability of a plane shear layer, where the velocity $\bar{V}$ is taken in the x-direction and varies linearly with z ($\bar{V}=z$) from $z=-1$ to $z=+1$. Outside the shear layer the velocity is constant ($\bar{V}=-1$ for $z<-1$ and $\bar{V}=+1$ for $z>+1$). Lengths and velocities are measured in units of half the thickness of the shear layer and the flow speed at the edge of the shear layer respectively. Sound speed a_0 and density $\bar{\varrho}$ are assumed to be constant (but not necessarily equal) outside and inside the shear layer and the Mach number M is defined as the ratio of the flow speed at the edge of the shear layer ($z=+1$) to the sound velocity within the shear layer.

Due to Squire's theorem (*cf.* Ray 1982) it is sufficient to consider two-dimensional perturbations proportional to $\sim\exp[ik(x+\omega t)]$, where k denotes the wavenumber and $\sigma=\omega k$ is the complex eigenfrequency. The linearized Euler equation for an adiabatic flow describing the evolution of the perturbations may then be condensed into the following equation for the Eulerian pressure perturbation $\tilde{p}$ (*cf.* Ray 1982):

$$\frac{d^2\tilde{p}}{dz^2}-\frac{2}{\bar{\sigma}}\frac{d\bar{\sigma}}{dz}\frac{d\tilde{p}}{dz}-k^2(1-M^2\bar{\sigma}^2)\,\tilde{p}=0 \tag{2.1}$$

where $\bar{\sigma}$ is defined as

$$\bar{\sigma}=\omega+\bar{V} \tag{2.2}$$

and the z-component of the velocity perturbation is given by

$$\tilde{v}_z=\frac{i}{k\bar{\sigma}}\frac{1}{\bar{\varrho}}\frac{d\tilde{p}}{dz}\,. \tag{2.3}$$

In the interval $z\in[-1,+1]$ we apply the transformation

$$Q=\bar{\sigma}^{-1/2}\tilde{p} \tag{2.4}$$

$$\zeta=ikM\bar{\sigma}^2 \tag{2.5}$$

and obtain from equation (2.1)

$$\frac{d^2Q}{d\zeta^2}+\left(-\frac{1}{4}+\frac{\varkappa}{\zeta}+\frac{\frac{1}{4}-\mu^2}{\zeta^2}\right)Q=0 \tag{2.6}$$

where

$$\varkappa=\frac{i}{4}\frac{k}{M}, \tag{2.7}$$

$$\mu=\frac{3}{4}\,. \tag{2.8}$$

Equation (2.5) is the standard form of Whittaker's equation, whose general solution can be given analytically in terms of confluent hypergeometric functions $M_{\varkappa,\mu}$ (see Abramowitz & Stegun 1970):

$$Q = c_1 M_{\varkappa,\mu}(\zeta) + c_2 M_{\varkappa,-\mu}(\zeta). \tag{2.9}$$

c_1 and c_2 are integration constants, whose ratio together with the pattern speed ω is determined by the boundary or matching conditions applied at $z = \pm 1$. We note that an equivalent analytical solution of the problem has been given in a different context by Goldstein & Rice (1973).

The solution of the perturbation equation (2.1) in the intervals $z \in (-\infty, -1]$ and $z \in [1, \infty)$ correspond to plane in- and outgoing sound waves which for the case of equal sound velocity inside and outside the shear layer are given by

$$Q = \exp[\pm k(1 - M^2\bar{\sigma}^2)^{1/2} z]. \tag{2.10}$$

3 Boundary conditions

Momentum balance and mass conservation require the pressure perturbation $\tilde{p}$ and the z-component of the velocity perturbation $\tilde{v}_z$ to be continuous, in particular at the boundaries of the shear layer ($z = \pm 1$). Since eigenfunctions are determined only up to a constant factor this condition is equivalent to the requirement that the ratios $\tilde{v}_z/\tilde{p}$ match at $z = \pm 1$, which for a continuous velocity profile $\bar{V}$ may be expressed as:

$$\frac{1}{\bar{\varrho}_{\text{in}}}\left(\frac{1}{\tilde{p}_{\text{in}}}\frac{d\tilde{p}_{\text{in}}}{dz}\right)\Bigg|_{z=\pm1} = \frac{1}{\bar{\varrho}_{\text{out}}}\left(\frac{1}{\tilde{p}_{\text{out}}}\frac{d\tilde{p}_{\text{out}}}{dz}\right)\Bigg|_{z=\pm1} \tag{3.1}$$

where subscripts 'in' and 'out' refer to quantities inside and outside the shear layer respectively.

In the following we shall consider three extreme cases of the condition (3.1): For $\bar{\varrho}_{\text{in}}/\bar{\varrho}_{\text{out}} \to \infty$ equation (3.1) is equivalent to $\tilde{p}_{\text{in}}|_{z=\pm1} = 0$, for $\bar{\varrho}_{\text{in}}/\bar{\varrho}_{\text{out}} \to 0$ to

$$\tilde{v}_{z,\text{in}}\Bigg|_{z=\pm1} \sim \frac{d\tilde{p}_{\text{in}}}{dz}\Bigg|_{z=\pm1} = 0.$$

If the density (and the sound velocity) outside and inside the shear layer are equal, a case considered by Ray (1982) and Choudhury & Lovelace (1984), the right-hand side of equation (3.1) has to be evaluated according to the solution (2.10), where the sign in equation (2.10) has to be chosen to ensure outgoing waves for $z < -1$ and $z > +1$.

In terms of the variable Q given by equation (2.9) the boundary conditions to be applied at $z = \pm 1$ may be expressed as

$$Q = 0 \tag{3.2}$$

if the pressure perturbation is required to vanish ($\bar{\varrho}_{\text{in}}/\bar{\varrho}_{\text{out}} \to \infty$), as

$$\frac{1}{Q}\frac{dQ}{d\zeta} + \frac{1}{4\zeta} = 0 \tag{3.3}$$

if the velocity perturbation is required to vanish ($\bar{\varrho}_{\text{in}}/\bar{\varrho}_{\text{out}} \to 0$), and as

$$\frac{1}{Q}\frac{dQ}{d\zeta} + \frac{1}{4\zeta} = \pm\frac{1}{2}\left(1 - \frac{4\varkappa}{\zeta}\right)^{1/2} \tag{3.4}$$

if the sound velocity is constant all over the flow and only outgoing sound waves are allowed at infinity. In equation (3.4) the upper sign has to be chosen at $z = -1$ and the lower sign at $z = +1$ to

ensure outgoing waves. We note that for the correct determination of the sign the radiation condition has to be applied in a frame of reference moving with the medium at infinity [for a detailed discussion see Ray (1982) or Glatzel (1987b)].

It is also possible to derive a radiation condition similar to equation (3.4) on the basis of a local solution of equation (2.6) only. The two fundamental local solutions of equation (2.6) may be characterized by

$$\frac{1}{Q}\frac{dQ}{d\zeta} = \pm\frac{1}{2}\left(1-\frac{4\varkappa}{\zeta}+\frac{5/4}{\zeta^2}\right)^{1/2} \tag{3.5}$$

where the upper sign corresponds to a sound wave travelling in the negative z-direction, the lower sign to a wave travelling in the positive z-direction. If we ask for solutions of the perturbation equation (2.1) which correspond to outgoing waves at $z=\pm1$ we may therefore regard equation (3.5) as the appropriate boundary condition where the signs are chosen as for equation (3.4).

For the derivation of the radiation condition (3.4) the discontinuity in the derivative of the velocity profile has been taken into account properly, whereas the regions with $|z|>1$ have been disregarded in the derivation of the condition (3.5). Equation (3.4) describes outgoing waves for $|z|\geqslant 1$, equation (3.5) for $|z|\approx 1$ on the basis of the solution for the linear velocity profile. Since the conditions (3.4) and (3.5) differ by a term of the order of $1/\zeta$ we conclude that there is a reflected sound wave for $|z|<1$ if the condition (3.4) is applied. This reflection must be due to the velocity profile, i.e. to the discontinuity of its gradient at $z=\pm1$, since the sound velocity is constant all over the flow. (For sound scattering by a shear layer see Koutsoyannis, Karamcheti & Galant 1980.) We shall comment on the consequences for the modal structure of the reflection of sound waves at $z=\pm1$ due to the velocity profile in Section 5.4.

4 Comparison with the rotating shear layer

In a previous paper (Glatzel 1987b) we have studied the modal structure of a rotating shear flow having constant sound speed and constant specific angular momentum distribution. In the limit of a thin shear layer, high Mach numbers M and high azimuthal wavenumbers m (the vertical wavenumber was taken to be zero) we have shown that the perturbation equation reduces to Whittaker's equation (see equation 2.6) with $\mu=\frac{1}{4}$ and $\varkappa=i/4[(m/2)/M]$. For the rotating shear layer the variables Q and ζ are given by $Q=\bar{\sigma}^{-1/2}\tilde{p}$ and $\zeta=i(m/2)M\bar{\sigma}^2$ where $\tilde{p}$ denotes the Eulerian pressure perturbation and $\bar{\sigma}$ is defined as $\bar{\sigma}=\omega+\Omega$. $\sigma=\omega m$ is the complex eigenfrequency and $\Omega\sim 1/r^2$ the unperturbed angular velocity. The dispersion relations had been derived for the boundary condition $Q=0$.

A comparison with Section 2 (equations 2.2–2.8) shows that the stability problem for the rotating flow studied previously is essentially the same as for the linear shear flow if we identify the wavenumber $m/2$ with k and the unperturbed angular velocity Ω with $\bar{V}$ (normalized by half of the thickness of the shear layer). A main consequence of the different μ is that the dispersion relations for zero pressure and zero velocity boundary condition have to be interchanged when comparing the rotating with the linear shear layer.

The close relation between the rotating and the linear shear layer means that rotation, i.e. angular momentum, centrifugal and Coriolis forces can at most modify but not be responsible for any instability found. A hint on the possible cause of the instabilities is given by the evolution equation for the positive definite perturbation energy $\tilde{E}$ which for the rotating flow is given by (see Glatzel 1987a):

$$\frac{\partial}{\partial t}r\langle\tilde{E}\rangle = r^2\bar{\varrho}\langle-\tilde{v}_r\tilde{v}_\phi\rangle\frac{d\Omega}{dr}-\frac{d}{dr}(r\langle\tilde{v}_r\tilde{p}\rangle). \tag{4.1}$$

$\tilde{v}_r$ and $\tilde{v}_\phi$ are the radial and tangential components of the velocity perturbation, $\langle\,\rangle$ denotes an angular average and $\tilde{E}$ is defined as:

$$\tilde{E} = \frac{1}{2}\,\bar{\varrho}(\tilde{v}_r^2+\tilde{v}_\phi^2)+\frac{1}{2}\,\frac{\tilde{p}^2}{\bar{\varrho}a_0^2}\,. \tag{4.2}$$

Similar equations where the angular velocity gradient is to be replaced by the velocity gradient also hold for the linear shear layer. The second term on the right-hand side of equation (4.1) represents the acoustic energy flux and merely corresponds to a redistribution of perturbation energy. The first term describes the production of perturbation energy associated with the Reynolds stress and is proportional to the shear both for the rotating and the linear shear layer. Thus we may conclude that the shear is the cause of the instabilities. However, according to equation (4.1) shear is not sufficient for an instability and a particular mechanism involving sound or surface waves (or any other sort of waves) is needed to produce an instability from the unstable tendency. These mechanisms have been discussed in detail in Glatzel (1987b) and according to the correspondence between the rotating and the linear shear layer they are also applicable to the linear shear layer.

5 Dispersion relations

5.1 GENERAL REMARKS

Exact dispersion relations are obtained by applying the various boundary conditions (3.2)–(3.5) at $z=\pm 1$ using the solution (2.9) of the perturbation equation. Formulae for derivatives and relations among the confluent hypergeometric functions $M_{\varkappa,\mu}$ and the related functions ${}_1F_1$ defined by

$$M_{\varkappa,\mu}(\zeta) = \exp(-\zeta/2)\,\zeta^{1/2+\mu}\,{}_1F_1(1/2+\mu-\varkappa;\,1+2\mu;\,\zeta) \tag{5.1}$$

may be found in Abramowitz & Stegun (1970). Algorithms for the calculation of the functions ${}_1F_1$ are given by Luke (1977). In the following subscripts '$_+$' and '$_-$' refer to the respective quantity evaluated at $z=+1$ and $z=-1$.

Since the results turn out to be – even quantitatively – very similar to the exact treatment and more physical insight is gained we shall also discuss the dispersion relations derived on the basis of an asymptotic expansion of the functions $M_{\varkappa,\mu}$ for $|\zeta_\pm| \to \infty$ (see Abramowitz & Stegun 1970):

$$\frac{M_{\varkappa,\mu}}{\Gamma(1+2\mu)} = \frac{\exp[i\pi(1/2+\mu-\varkappa)]}{\Gamma(1/2+\mu+\varkappa)}\exp(-\zeta/2)\,\zeta^{\varkappa}A + \frac{1}{\Gamma(1/2+\mu-\varkappa)}\exp(\zeta/2)\,\zeta^{-\varkappa}B \tag{5.2}$$

with

$$A=1-(1/2+\mu-\varkappa)(1/2-\mu-\varkappa)/\zeta+O(1/\zeta^2) \tag{5.3}$$

and

$$B=1+(1/2+\mu+\varkappa)(1/2-\mu+\varkappa)/\zeta+O(1/\zeta^2). \tag{5.4}$$

As discussed in a previous paper (Glatzel 1987b) this expansion of $M_{\varkappa,\mu}$ has to be multiplied by $\exp[i2\pi(1/4+\mu)]$, if ζ passes the negative imaginary axis. Accordingly, this factor has to be taken into account, if a critical layer occurs within the flow, i.e. if $\mathscr{R}\bar{\sigma}=0$ at some $|z|<1$.

It is particularly obvious that the solution (2.9) of the perturbation equation may be interpreted as the superposition of incoming and outgoing waves, if $M_{\varkappa,\mu}$ is represented by its asymptotic expansion (equations 5.2–5.4).

In the limit of low Mach numbers an expansion of $M_{\varkappa,\mu}$ in terms of Bessel functions J_ν will be used (*cf.* Luke 1969):

$$M_{\varkappa,\mu}(\zeta) = \zeta^{1/2}\varkappa^{-\mu}\Gamma(2\mu+1)\sum_{n=0}^{\infty} A_n \left(\frac{\zeta}{4\varkappa}\right)^{n/2} J_{2\mu+n}(\sqrt{4\varkappa\zeta}) \tag{5.5}$$

with

$$A_0=1, \quad A_1=0, \quad A_2=1/2+\mu \tag{5.6}$$

and

$$(n+1)A_{n+1} = (n+2\mu)A_{n-1} - 2\varkappa A_{n-2}. \tag{5.7}$$

The expansion (5.5) is essentially a power series in the Mach number M, which for $M=0(|\varkappa| \to \infty)$ yields the solution Q of the perturbation equation as

$$Q = c_1\bar{\sigma}J_{3/2}(ik\bar{\sigma}) + c_2\bar{\sigma}J_{-3/2}(ik\bar{\sigma}). \tag{5.8}$$

Q as given by equation (5.8) is simply the solution of the incompressible perturbation equation.

5.2 PERFECTLY REFLECTING BOUNDARIES

Using the lowest order terms of the asymptotic expansion (5.2)–(5.4) only and assuming a critical layer within the flow the following approximate dispersion relation is found, if the pressure perturbation (upper sign) or the velocity perturbation (lower sign) is required to vanish at both boundaries:

$$\exp(-\zeta_-)\,\zeta_-^{2\varkappa}\exp(-i\pi\varkappa \pm i\pi/2)\left[\frac{\Gamma(-1/4-\varkappa)\,\Gamma(5/4-\varkappa)}{\Gamma(-1/4+\varkappa)\,\Gamma(5/4+\varkappa)}\right]^{1/2} = R_-(\zeta_+) \tag{5.9}$$

or, equivalently

$$\exp(-\zeta_+)\,\zeta_+^{2\varkappa}\exp(-i\pi\varkappa \pm i\pi/2)\left[\frac{\Gamma(-1/4-\varkappa)\,\Gamma(5/4-\varkappa)}{\Gamma(-1/4+\varkappa)\,\Gamma(5/4+\varkappa)}\right]^{1/2} = R_+(\zeta_-) \tag{5.10}$$

with

$$R_- = -\frac{[1+\exp(-\pi k/M)]^{1/2} - R_+}{[1+\exp(-\pi k/M)]^{1/2}R_+ - 1} \tag{5.11}$$

and

$$R_+ = -\frac{[1+\exp(-\pi k/M)]^{1/2} - R_-}{[1+\exp(-\pi k/M)]^{1/2}R_- - 1}. \tag{5.12}$$

By taking the logarithm of equation (5.9) and (5.10) and multiplying them we get

$$\left[\left[\bar{\sigma}_-^2 - \frac{1}{kM}\left\{\pi(2n_- \pm 1/2) + \frac{2\varkappa}{i}\log(kM\bar{\sigma}_-^2) - \arg[\Gamma(-1/4+\varkappa)\,\Gamma(5/4+\varkappa)]\right\}\right]\right]$$
$$\times\left[\left[\bar{\sigma}_+^2 - \frac{1}{kM}\left\{\pi(2n_+ \pm 1/2) + \frac{2\varkappa}{i}\log(kM\bar{\sigma}_+^2) - \arg[\Gamma(-1/4+\varkappa)\,\Gamma(5/4+\varkappa)]\right\}\right]\right]$$
$$= -\frac{1}{(kM)^2}\log R_-\log R_+ \tag{5.13}$$

where $n_\pm$ are integers satisfying $2n_\pm \pm 1/2 > 0$. The dispersion relation is valid for large $|\zeta_\pm|$, i.e. for large values of the product kM. Within this approximation the right-hand side of equation (5.13) can be assumed to be small compared with the expressions in double brackets and an approximate solution of equation (5.13) is given by the zero of each of the double brackets provided they have no common zero. These solutions describe two sets of neutral modes characterized by n_+ and n_- which belong to the boundary at $z=+1$ and $z=-1$ respectively. For small values of the ratio k/M they reduce to the remarkably simple dispersion relations:

$$\bar{\sigma}_- = \omega_- - 1 = -\left[\frac{\pi}{kM}(2n_- \pm 1/2)\right]^{1/2} \tag{5.14}$$

$$\bar{\sigma}_+ = \omega_+ + 1 = +\left[\frac{\pi}{kM}(2n_+ \pm 1/2)\right]^{1/2}. \tag{5.15}$$

The sign in front of the root is chosen to ensure a critical layer within the flow in accordance with our assumptions. As already mentioned this approximation does not hold, if the double brackets in equation (5.13) have a common zero, i.e. if a mode crossing occurs ($\omega_+ = \omega_-$). Using a procedure outlined by Cairns (1979) (see also Craik 1985) the details of the treatment of mode crossings have been given in a previous paper (Glatzel 1987b). Following the analysis and notation of Glatzel (1987b) an approximate solution of equation (5.13) near a mode crossing of any of the modes described by the decoupled dispersion relations denoted by $D_+(\omega)$ and $D_-(\omega)$, which are the expressions in the two double brackets of equation (5.13), is given by

$$\omega = \omega_+ + \frac{\omega_- - \omega_+}{2} \pm \left[\frac{(\omega_- - \omega_+)^2}{4} + \frac{\varepsilon(\omega_+ = \omega_-)}{(\partial D_+/\partial\omega)|_{\omega_+=\omega_-}\,(\partial D_-/\partial\omega)|_{\omega_-=\omega_+}}\right]^{1/2} \tag{5.16}$$

where ω_+ and ω_- are any solutions of the decoupled dispersion relations $D_+(\omega_+)=0$ and $D_-(\omega_-)=0$ and $\varepsilon(\omega_+=\omega_-)$ is the right-hand side of equation (5.13) evaluated at the crossing point.

ω_+ and ω_- can also be determined by equation (5.9) and (5.10) with $R_\pm = 1$. Therefore $R_\pm = 1$ has to be inserted on the right-hand side of equations (5.11) and (5.12) in order to calculate R_+ and R_- at a mode crossing:

$$R_+(\omega_+ = \omega_-) = R_-(\omega_+ = \omega_-) = \exp(i\pi). \tag{5.17}$$

Accordingly,

$$\varepsilon(\omega_+ = \omega_-) = \left(\frac{\pi}{kM}\right)^2 \tag{5.18}$$

is positive and independent of the particular mode crossing. The derivatives of the decoupled dispersion relations D_+ and D_- are found from equation (5.13) as:

$$\frac{\partial D_\pm}{\partial\omega} = -2\bar{\sigma}_\pm + \frac{1}{M^2\bar{\sigma}_\pm} \tag{5.19}$$

with

$$\frac{\partial D_\pm}{\partial\omega} \to -2\bar{\sigma}_\pm \qquad \text{for} \quad |\varkappa| \to 0. \tag{5.20}$$

According to equation (5.19) $\partial D_\pm/\partial\omega$ changes its sign at $|\bar{\sigma}_\pm| = (\sqrt{2}/2)\,(1/M)$.

If the second term in square brackets in equation (5.16) is positive, the mode crossing unfolds into an avoided crossing of neutral modes, otherwise into a band of instability (see Glatzel

1987b). Since ε is positive this means that the sign of the derivatives of the decoupled dispersion relations as given by equation (5.19) determines the stability behaviour. For all modes with $2n_{\pm}\pm 1/2>0$ having a critical layer within the flow the derivatives $\partial D_+/\partial\omega$ and $\partial D_-/\partial\omega$ have opposite sign and all mode crossings unfold into bands of instabilities. This is particularly obvious in the limit $|\varkappa| \to 0$ where equations (5.20), (5.14) and (5.15) hold. For the maximum growth rate $\mathcal{I}\sigma$ ($\sigma=\omega k$) at a mode crossing we find in this limit approximately:

$$|\mathcal{I}\sigma| = \frac{1}{2}\left(\frac{\pi k}{M}\right)^{1/2}[(2n_-\pm 1/2)(2n_+\pm 1/2)]^{-1/4}. \tag{5.21}$$

Compared with the growth rates obtained from the dispersion relation (5.9) the growth rate according to equation (5.21) is too high by a factor of ≈ 3, which seems to be due to the interaction of different instability bands. Equation (5.21) may also be expressed as a function of the wavenumber and the integers n_+ and n_- only:

$$|\mathcal{I}\omega|^{-1} = \tfrac{1}{2}[(4n_+\pm 1)^{1/2}+(4n_-\pm 1)^{1/2}][(4n_+\pm 1)^{1/2}(4n_-\pm 1)^{1/2}]^{1/2}. \tag{5.22}$$

Equations (5.21) and (5.22) are valid in the limit $|k/M| \to 0$.

To illustrate the behaviour described above we have plotted the eigenfrequencies of the various modes for the wavenumber $k=1$ as a function of the Mach number M in Figs 1–6. In this case the corrections for finite wavenumbers, i.e. the terms involving the Γ-functions and the logarithms in equation (5.13), are small and we can use the approximations for $|\varkappa| \to 0$. For high wavenumbers the correction terms prevent the modes having a critical layer within the flow and $n_{\pm}\neq 0$ to extend into the subsonic regime. Moreover, they reduce the bandwidth of the instability bands. However, apart from these modifications the qualitative behaviour is the same as for low wavenumbers.

The two sets of neutral modes corresponding to $D_+(\omega_+)=0$ and $D_-(\omega_-)=0$ are plotted in Fig. 1 for zero velocity and in Fig. 4 for zero pressure perturbation at the boundaries. The main difference between the two boundary conditions lies in the non-existence of the modes having

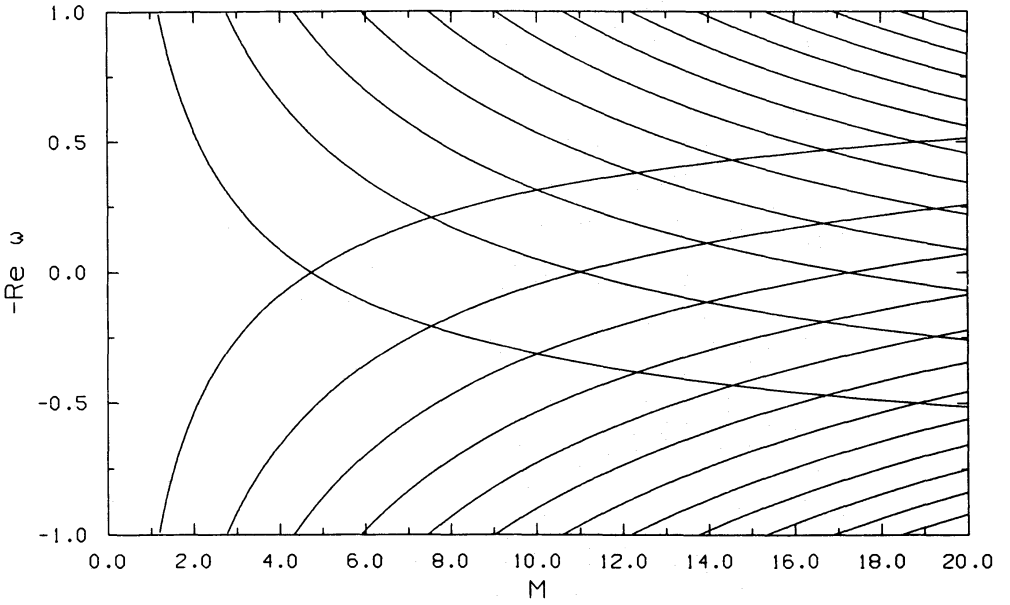

Figure 1. The pattern speeds $-\mathcal{R}\omega$ of the two sets of neutrally stable decoupled modes belonging to the boundaries at $z=+1$ and $z=-1$ as a function of the Mach number M for wavenumber $k=1$. Zero velocity perturbation has been required at the boundaries.

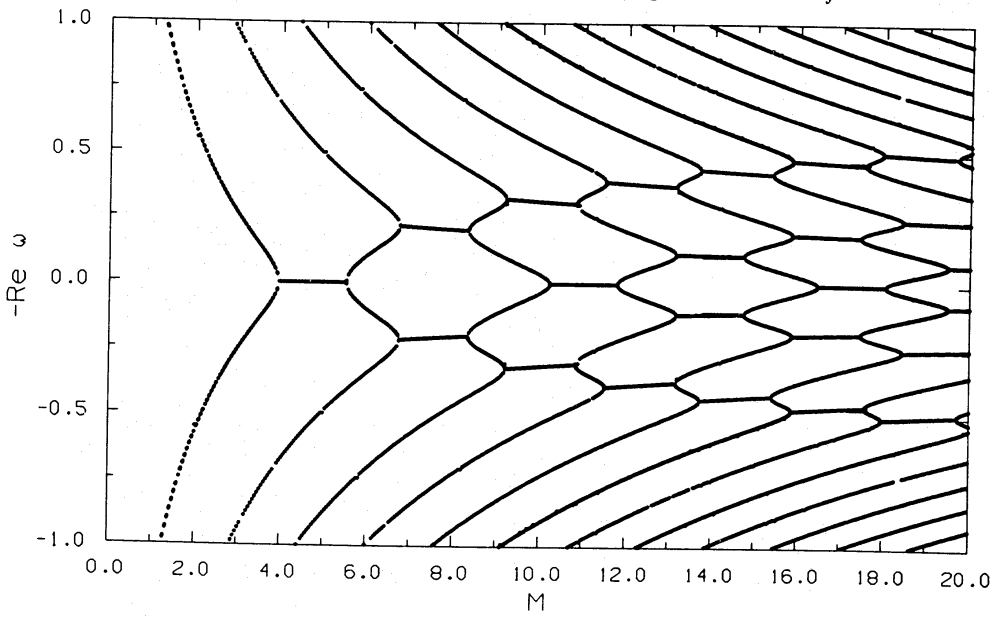

(a)

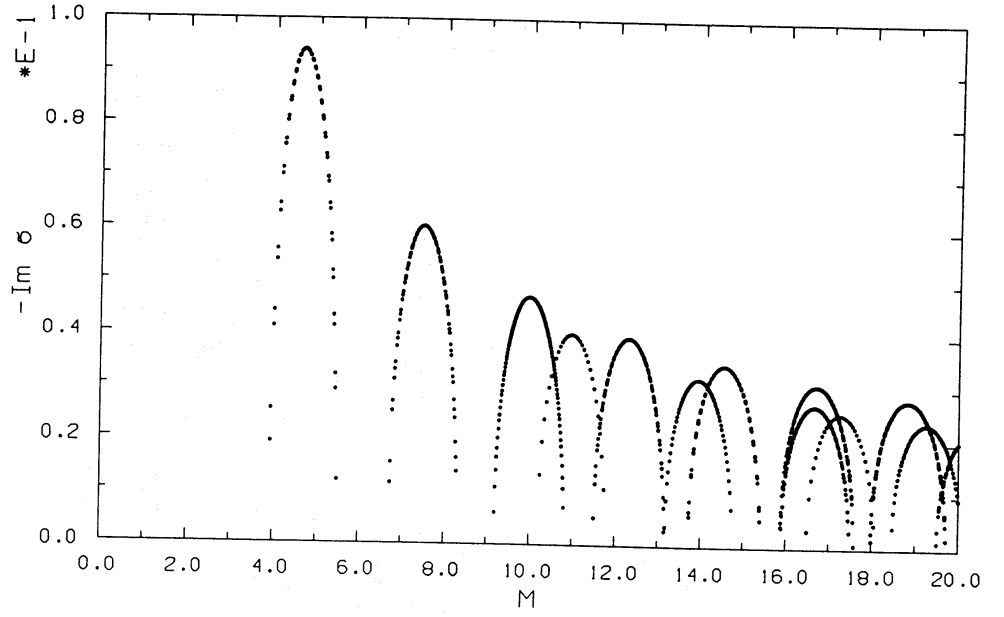

(b)

Figure 2. Pattern speeds $-\mathscr{R}\omega$ and growth rates $-\mathscr{I}\sigma$ as a function of the Mach number M for zero velocity perturbation at the boundaries and wavenumber $k=1$ according to the approximate dispersion relation (5.9) or (5.10).

$n_{\pm}=0$ for the condition of zero velocity perturbation (see also equations 5.14 and 5.15). Their strong dependence on the boundary condition as well as the fact that only these modes extend into the subsonic regime indicates that they are physically different from modes with $n_{\pm}>0$.

We have plotted the eigenfrequencies according to the analytical dispersion relation (5.9) or (5.10) in Fig. 2 (zero velocity perturbation) and Fig. 5 (zero pressure perturbation). A comparison with Figs 1 and 4 shows that the decoupled neutral modes are in fact a reasonable approximation to the full problem except near mode crossings. Moreover, in agreement with our predictions all mode crossings have unfolded into bands of instabilities. For high Mach numbers the instability bands merge (see Fig. 4) thus forming continuously unstable modes.

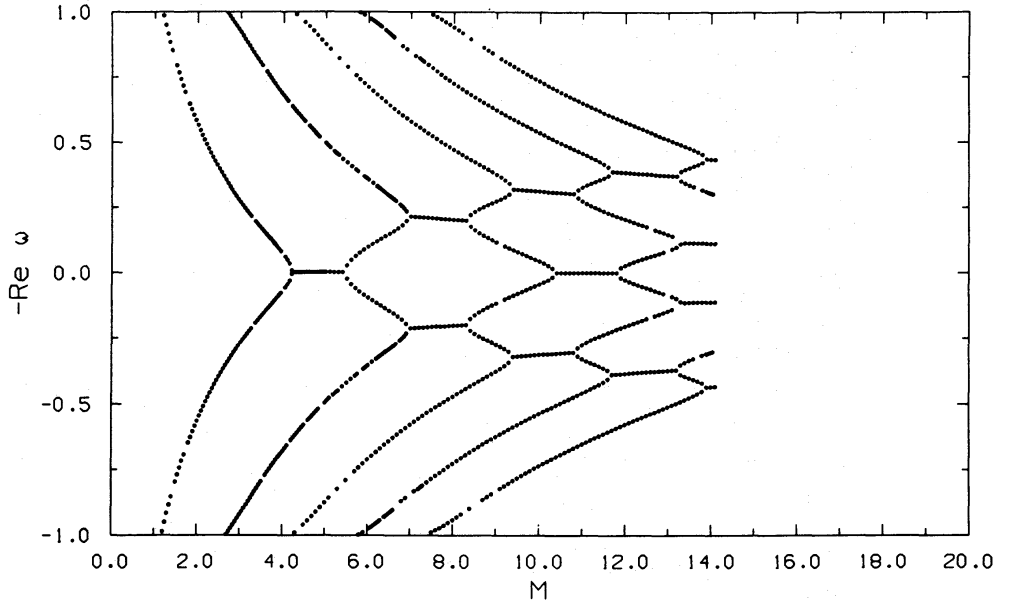

(a)

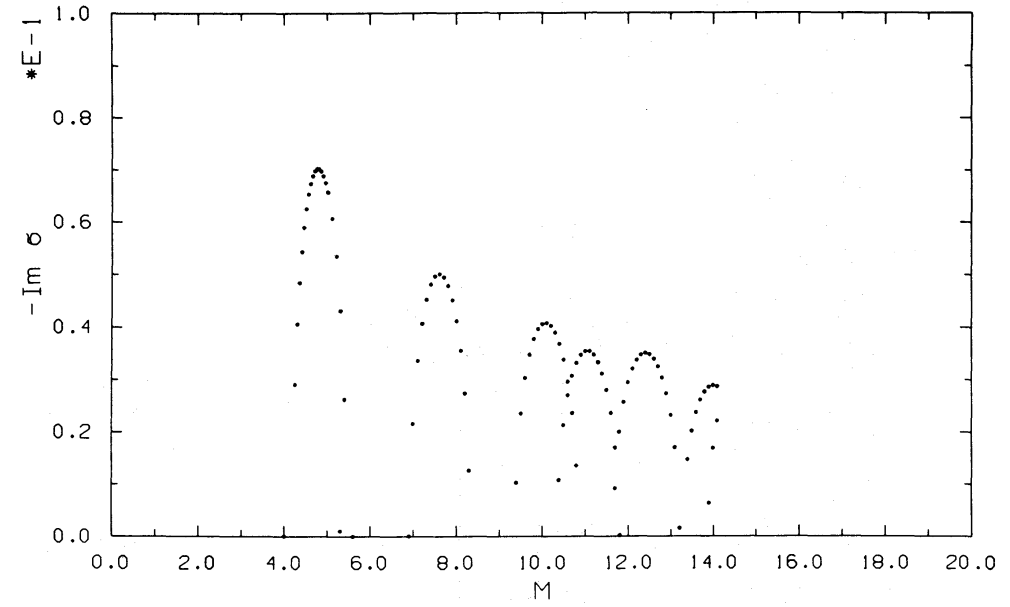

(b)

Figure 3. Same as Fig. 2 but according to the exact dispersion relation (5.23).

For comparison with the approximate analytical treatment the eigenfrequencies according tc the corresponding exact dispersion relations are plotted in Figs 3 and 6, where the exac dispersion relation for zero velocity perturbation at the boundaries is given by:

$$\bar{\sigma}_-^3 \frac{(2\zeta_-+1-4\varkappa)\,{}_1F_1(5/4-\varkappa, 5/2, \zeta_-)+(4\varkappa+5)\,{}_1F_1(1/4-\varkappa, 5/2, \zeta_-)}{(2\zeta_-+1-4\varkappa)\,{}_1F_1(-1/4-\varkappa, -1/2, \zeta_-)+(4\varkappa-1)\,{}_1F_1(-5/4-\varkappa, -1/2, \zeta_-)}$$

$$-\bar{\sigma}_+^3 \frac{(2\zeta_++1-4\varkappa)\,{}_1F_1(5/4-\varkappa, 5/2, \zeta_+)+(4\varkappa+5)\,{}_1F_1(1/4-\varkappa, 5/2, \zeta_+)}{(2\zeta_++1-4\varkappa)\,{}_1F_1(-1/4-\varkappa, -1/2, \zeta_+)+(4\varkappa-1)\,{}_1F_1(-5/4-\varkappa, -1/2, \zeta_+)} = 0. \quad (5.23$$

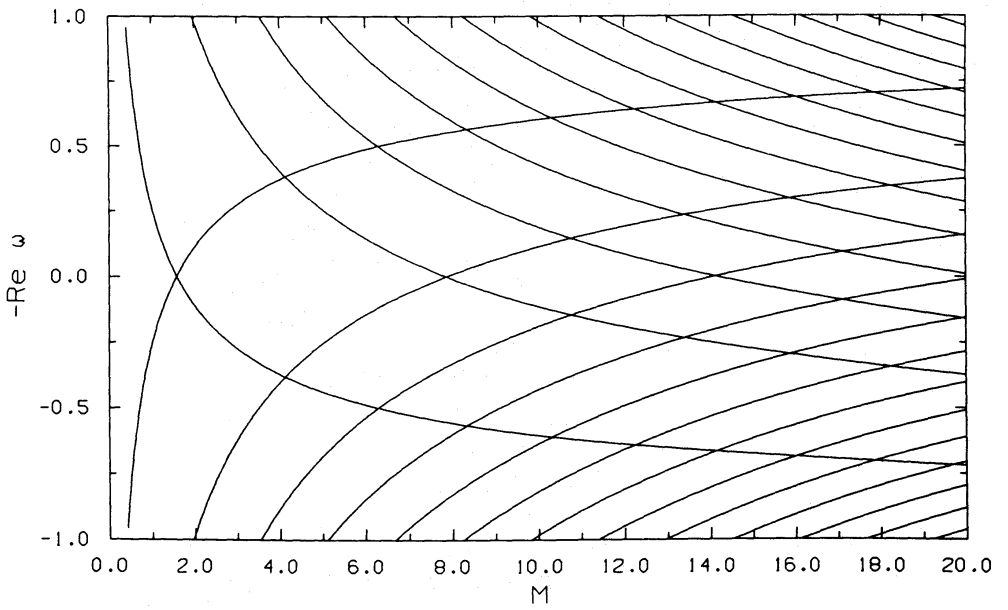

Figure 4. Same as Fig. 1 but for zero pressure perturbation at the boundaries.

For zero pressure perturbation at the boundaries we obtain:

$$\bar{\sigma}_-^3 \frac{{}_1F_1(5/4-\varkappa,\ 5/2,\ \zeta_-)}{{}_1F_1(-1/4-\varkappa,\ -1/2,\ \zeta_-)} - \bar{\sigma}_+^3 \frac{{}_1F_1(5/4-\varkappa,\ 5/2,\ \zeta_+)}{{}_1F_1(-1/4-\varkappa,\ -1/2,\ \zeta_+)} = 0. \tag{5.24}$$

The agreement between the exact eigenfrequencies (Figs 3 and 6) and the analytical approximations (Figs 2 and 5) is reasonable at high Mach numbers but becomes less satisfactory for low Mach numbers and if the critical layers of the modes get close to the boundary to which they belong. This is because the asymptotic expansion used for the derivation of the analytical dispersion relation is valid for $|\zeta| \to \infty$, i.e. for high Mach numbers and large distances of the critical layer from the boundaries. For modes having $n_\pm > 0$ the real parts of the eigenfrequencies are in reasonable agreement even for low Mach numbers, whereas the growth rates of the instabilities are somewhat smaller in the exact treatment for low Mach numbers. For the two modes with $n_\pm = 0$, which only occur for zero pressure perturbation at the boundaries and whose critical layer is closest to their corresponding boundary, the critical layer is shifted towards the boundaries and the instability bands are shifted towards lower Mach numbers when compared with the approximate treatment. The growth rates of the instabilities are in reasonable agreement and the merging of bands as found in Fig. 5 is even more pronounced in the exact treatment (Fig. 6).

For $M \to 0$ the analytical approximation fails, which gives rise to a qualitative difference between the approximate and the exact treatment: The instability band due to the crossing of the modes with $n_+ = 0$ and $n_- = 0$ extends to $M = 0$ attaining its maximum growth rate there in the exact treatment (*cf.* Fig. 6), whereas in the approximation the corresponding instability band with a slightly higher maximum growth rate splits into two neutral modes again for $M \to 0$ (see Fig. 5). Within the exact treatment the $n_\pm = 0$ modes do not cross unfolding into a band of instability for wavenumbers $k > 1.2$. Rather they remain neutral for $M \to 0$ with a finite limit for ω in the range $0 < |\omega| < 1$. This behaviour again indicates a different physical nature of the $n_\pm = 0$ modes. We shall discuss the limit $M \to 0$ in detail in Section 5.5.

The case when no critical layer occurs within the flow remains to be studied. As for rotating flows (*cf.* Papaloizou & Pringle 1985) it is possible to show for the boundary condition of zero

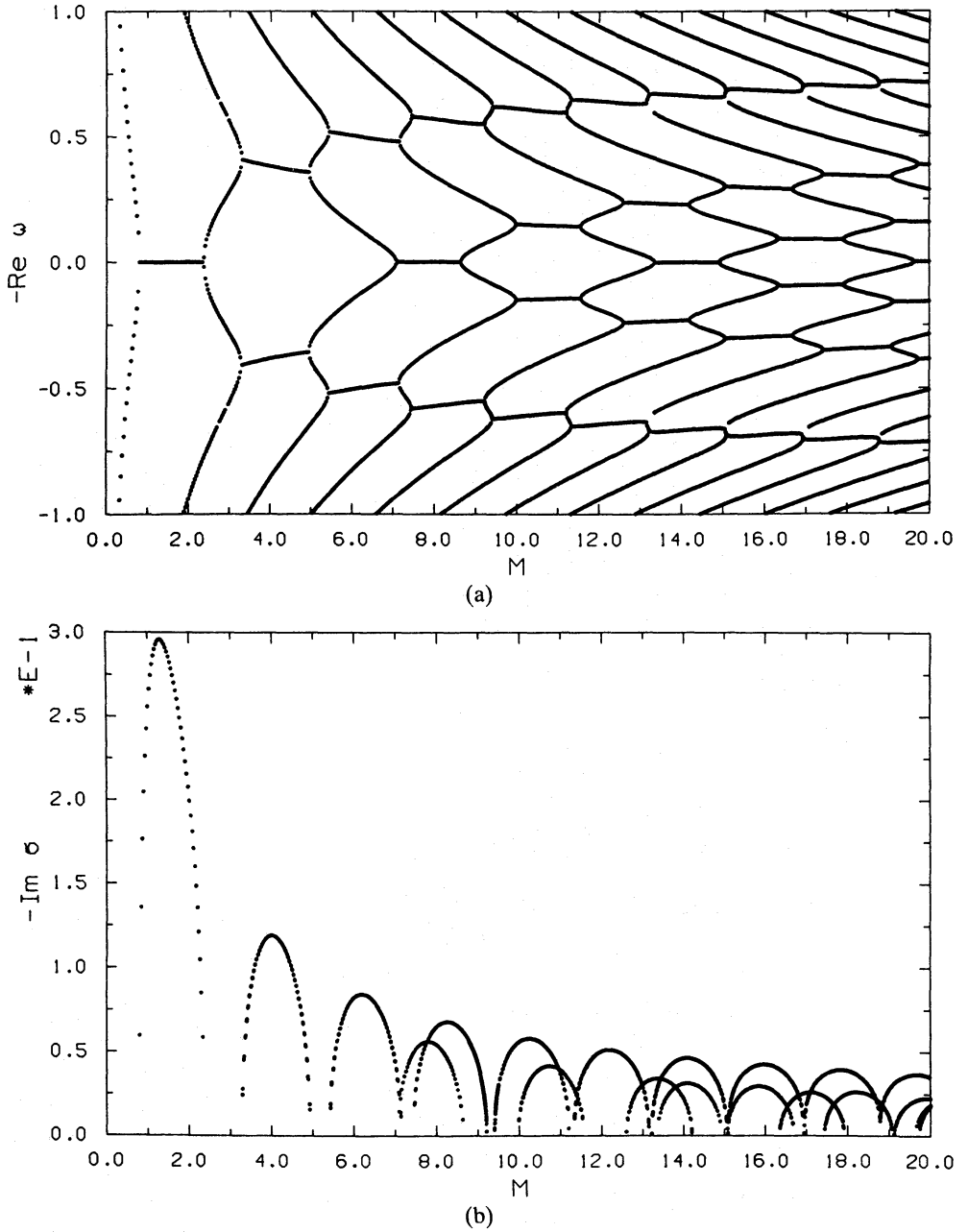

Figure 5. Same as Fig. 2 but for zero pressure perturbation at the boundaries.

velocity or pressure perturbation that any mode having a non-zero growth or damping rate must have a critical layer within the flow. Accordingly, a mode having no critical layer within the flow must be neutrally stable. Using again the lowest order terms of the asymptotic expansion (5.2)–(5.4) we obtain the following dispersion relation both for zero velocity and zero pressure perturbation at the boundaries:

$$\omega + \frac{1}{4M^2} \log \frac{\omega - 1}{\omega + 1} = \frac{\pi}{2} \frac{1}{M} \frac{n}{k} \tag{5.25}$$

where n is an integer. For $|\varkappa| \to 0$ the dispersion relation reduces to:

$$\omega = \frac{\pi}{2} \frac{1}{M} \frac{n}{k} . \tag{5.26}$$

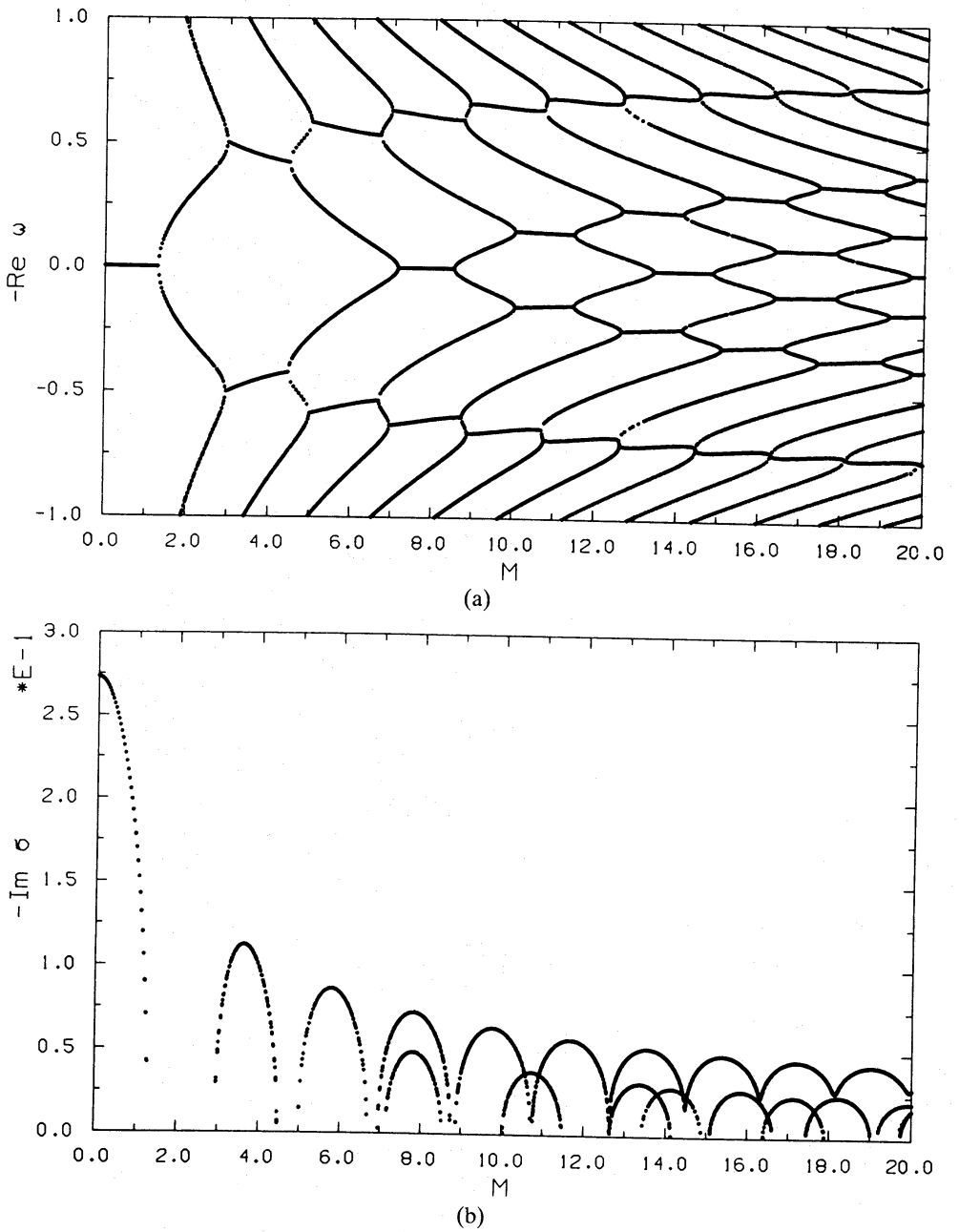

Figure 6. Same as Fig. 2 but for zero pressure perturbation at the boundaries and according to the exact dispersion relation (5.24).

Since we assumed that no critical layer occurs within the flow the solutions of (5.25) and (5.26) are restricted to $|\omega|>1$. Moreover, the validity of the asymptotic expansions (5.2)–(5.4) for $|\zeta| \to \infty$ requires $|\omega| \gg 1$, which can be achieved by choosing $|n|$ sufficiently large for given k, M. With n and ω restricted in this way the solutions of equation (5.25) describe two sets of neutral modes having positive and negative n respectively. These two sets are the direct continuation for $|\omega|>1$ of the two sets of neutral modes having a critical layer within the flow and $n_{\pm} \geq 1$ which approach $|\omega|=1$ from below (see Figs 1–6). However, since the asymptotic expansion used for the derivation of equation (5.25) is not valid in the vicinity of $|\omega| \approx 1$ the exact dispersion relations (5.23) and (5.24) have to be used there to verify this connection explicitly.

In the limit $k \to 0$ the modes having $n_{\pm} \geq 1$ disappear (*cf.* equations 5.14, 5.15 and 5.26). For the condition of zero pressure perturbation at the boundaries the behaviour of the modes with $n_{\pm}=0$

is found from equation (5.24): As k tends to zero at a fixed Mach number M we have $\omega^2 \to -1/3$, i.e. the first instability band becomes independent of the Mach number.

5.3 ONE PERFECTLY REFLECTING BOUNDARY

If we require the pressure perturbation (upper sign) or the velocity perturbation (lower sign) to vanish at one boundary we obtain an approximate dispersion relation using the lowest order terms of the asymptotic expansion (5.2)–(5.4):

$$\exp(-\zeta)\,\zeta^{2\varkappa}\exp(-i\pi\varkappa \pm i\pi/2)\left[\frac{\Gamma(-1/4-\varkappa)\,\Gamma(5/4-\varkappa)}{\Gamma(-1/4+\varkappa)\,\Gamma(5/4+\varkappa)}\right]^{1/2}$$

$$= \frac{1-\frac{8}{3}\frac{c_2}{c_1}\frac{\Gamma(5/4-\varkappa)}{\Gamma(-1/4-\varkappa)}}{\exp(-i\pi/4)\left\{\frac{\sin[\pi(-1/4-\varkappa)]}{\sin[\pi(-1/4+\varkappa)]}\right\}^{1/2} - \exp(i\pi/4)\,\frac{8}{3}\frac{c_2}{c_1}\frac{\Gamma(5/4-\varkappa)}{\Gamma(-1/4-\varkappa)}\left\{\frac{\sin[\pi(-1/4+\varkappa)]}{\sin[\pi(-1/4-\varkappa)]}\right\}^{1/2}}$$

$$= \frac{\left\{\frac{\sin[\pi(-1/4+\varkappa)]}{\sin[\pi(-1/4-\varkappa)]}\right\}^{1/2} - \frac{8}{3}\frac{c_2}{c_1}\frac{\Gamma(5/4+\varkappa)}{\Gamma(-1/4+\varkappa)}\left\{\frac{\sin[\pi(-1/4-\varkappa)]}{\sin[\pi(-1/4+\varkappa)]}\right\}^{1/2}}{\exp(-i\pi/4)-\exp(i\pi/4)\,\frac{8}{3}\frac{c_2}{c_1}\frac{\Gamma(5/4+\varkappa)}{\Gamma(-1/4+\varkappa)}}. \tag{5.27}$$

In equation (5.27) ζ is to be evaluated at the boundary where the pressure or the velocity perturbation is required to vanish and the ratio c_2/c_1 of the integration constants has to be determined by the second boundary condition. We note the similarity of equation (5.27) and equations (5.9) and (5.10).

For a suitable choice of the ratio c_2/c_1, i.e. by adopting an appropriate boundary condition at the second boundary, the right-hand side of equation (5.27) becomes equal to unity. Physically this boundary condition means that the acoustic energy flux is zero, even if the pressure and the velocity perturbation do not vanish (see Glatzel 1987b). The dispersion relation obtained in this way yields a set of neutral modes associated with the boundary where the pressure or the velocity perturbation has been required to vanish. Furthermore, these modes are identical with the neutral decoupled modes discussed in Section 5.2 and plotted in Figs 1 and 4. This example shows that one perfectly reflecting boundary is not sufficient for an instability.

Applying the radiation condition (3.4) at one of the boundaries we find for the ratio c_2/c_1 within the same approximation as above:

$$-\frac{8}{3}\frac{c_2}{c_1}\frac{\Gamma(5/4\pm\varkappa)}{\Gamma(-1/4\pm\varkappa)} = \exp(i3\pi/4 \mp i\pi/4) \tag{5.28}$$

where the signs in equation (5.28) have to be chosen as in equation (3.4). We note that to this order of the approximation the alternative radiation condition (3.5) also leads to the condition (5.28). The boundary conditions (5.27) and (5.28) may now be combined to derive a dispersion relation.

Assuming that there is no critical layer within the flow equation (5.28) is inserted into equation (5.27) but no physically meaningful solution can be obtained, since the right-hand side of equation (5.27) vanishes or becomes infinite. Thus we conclude that there is, at least within our approximation, no discrete mode having no critical layer within the flow.

According to Section 5.1 the expansion of $M_{\varkappa,-3/4}$ has to be multiplied with -1, if a critical layer is passed. In other words, the sign in front of c_2/c_1 has to be changed either in equation (5.27) or in

equation (5.28) if we insert equation (5.28) into equation (5.27) and assume the existence of a critical layer between the boundaries. In this case we obtain the dispersion relation:

$$\bar{\sigma}^2 - \frac{1}{kM}\left\{\pi(2n\pm 1/2) + \frac{2\varkappa}{i}\log(kM\bar{\sigma}^2) - \arg[\Gamma(-1/4+\varkappa)\,\Gamma(5/4+\varkappa)]\right\}$$

$$= \mp\frac{i}{2kM}\log[1+\exp(-\pi k/M)]. \tag{5.29}$$

The upper sign on the left-hand side of equation (5.29) corresponds to zero pressure perturbation, the lower to zero velocity perturbation at the boundary where $\bar{\sigma}$ is evaluated. The choice of signs on the right-hand side is the same as in equation (3.4).

The real parts of the eigenfrequencies given by equation (5.29) are essentially the same as for the neutral modes obtained with a zero right-hand side in equation (5.29). These modes are identical with the neutral modes obtained above for a suitable choice of the integration constants, for which the energy flux from the shear layer vanishes, and with the neutral decoupled modes discussed in Section 5.2 (see Figs 1 and 4). They seem to form the basic constituents of any of the dispersion relations.

The imaginary right-hand side of equation (5.29) causes the modes to become unstable, if the sign is chosen according to an outgoing wave. On the other hand, the same modes are damped, if the radiation condition is changed from an outgoing to an incoming wave. In other words, energy loss due to acoustic radiation destabilizes, energy supply stabilizes the system and zero energy flux yields neutral oscillations (provided there are no resonances, see also Glatzel 1987b). For $M \to 0$ the effect of acoustic radiation diminishes and the imaginary parts of the eigenfrequencies tend to zero as $k/M \to \infty$. In the limit of high Mach numbers ($|\varkappa| \to 0$) we find from equation (5.29) for the growth rate $\Im\sigma$ of the instability approximately:

$$|\Im\sigma| \approx \frac{\log[1+\exp(-\pi k/M)]}{2\pi}\,\frac{1}{2}\left(\frac{\pi k}{M}\right)^{1/2}(2n\pm 1/2)^{-1/2}. \tag{5.30}$$

Comparing equations (5.21) and (5.30) we conclude that the radiation instability is slightly weaker than the resonance instability.

5.4 PARTIALLY REFLECTING BOUNDARIES

We consider now the case where the sound velocities outside and inside the shear layer are equal. The appropriate boundary condition for both boundaries is then given by equation (3.4), which for $|\zeta| \to \infty$ reduces to equation (5.28). We emphasize that in this limit the alternative radiation condition (3.5) also reduces to equation (5.28). Since the eigenfrequency does not appear in equation (5.28) we cannot derive a dispersion relation by applying equation (5.28) at both boundaries. Moreover, c_2/c_1 is overdetermined and we obtain either trivial results or contradictions. Thus we conclude that the discrete spectrum is empty. This is not surprising, since an infinite configuration having constant sound velocity does not allow for reflection of sound waves and standing sound waves cannot exist. However, for the derivation of equation (5.28) from equation (3.4) (or 3.5) only the lowest order terms of the asymptotic expansion (5.2)–(5.4) have been used and it might be that a discrete spectrum appears, if we include higher order terms. We shall therefore study in the following the dispersion relations including terms of the order of $1/\zeta$ both in the expansion (5.2)–(5.4) and the radiation condition (3.4) and (3.5).

Even in the higher approximation we arrive at equation (5.28) if we apply the radiation condition (3.5). The discrete spectrum is still empty indicating that there is no sufficient internal

reflection of sound waves to produce standing sound waves. In comparing the radiation conditions (3.4) and (3.5) we have already mentioned in Section 3 that a reflection of sound waves by the velocity profile, i.e. by the discontinuity of its gradient at $z = \pm 1$, is neglected in the radiation condition (3.5) but is properly taken into account in the condition (3.4). As a consequence the conditions (3.4) and (3.5) differ by a term of the order of $1/\zeta$ describing the reflection of sound waves by the velocity profile. We shall show in the following that this reflection of sound waves by the velocity profile itself is in fact sufficient to produce a discrete spectrum. Thereby we shall discuss the dispersion relations for simplicity in the limit $|\varkappa| \to 0$, since the results are even quantitatively similar to the general case.

Applying the radiation condition (3.4) at both boundaries we obtain using the expansion (5.2)–(5.4) and including terms up to the order of $1/\zeta$

$$\omega = \frac{\pi}{2}\frac{1}{M}\frac{n}{k} + \frac{i}{2kM}\log\left[4kM(\omega^2-1)\right] \tag{5.31}$$

if no critical layer occurs within the flow, i.e. the integer n has to be chosen sufficiently large. We note the similarity of equation (5.31) and equation (5.26). The structure and the real parts of the eigenfrequencies are similar but all modes described by equation (5.31) are damped, whereas the modes given by equation (5.26) are neutrally stable. If a critical layer occurs within the flow we find the dispersion relation:

$$\zeta_- \exp(-\zeta_-)\exp(-i\pi/2) = \frac{\sqrt{2}-8\zeta_+ \exp(\zeta_+)\exp(-i\pi/2)}{8-16\sqrt{2}\zeta_+ \exp(\zeta_+)\exp(-i\pi/2)} = R_-(\zeta_+) \tag{5.32}$$

or

$$\zeta_+ \exp(\zeta_+)\exp(-i\pi/2) = \frac{\sqrt{2}-8\zeta_- \exp(-\zeta_-)\exp(-i\pi/2)}{8-16\sqrt{2}\zeta_- \exp(-\zeta_-)\exp(-i\pi/2)} = R_+(\zeta_-). \tag{5.33}$$

Using the same procedure as in Section 5.2 we obtain from equations (5.32) and (5.33):

$$\left\{\bar{\sigma}_-^2 - \frac{1}{kM}\left[\pi 2n_- - i\log(kM\bar{\sigma}_-^2)\right]\right\}\left\{\bar{\sigma}_+^2 - \frac{1}{kM}\left[\pi 2n_+ + i\log(kM\bar{\sigma}_+^2)\right]\right\}$$

$$= \frac{1}{(kM)^2}\log R_- \log R_+; \qquad n_\pm = 0, 1, 2, \ldots . \tag{5.34}$$

As in the case of perfectly reflecting boundaries the dispersion relation (5.34) may be interpreted as the superposition of two sets of modes belonging to the boundary at $z = +1$ and $z = -1$ respectively and given by the zero of each of the expressions in curly brackets in equation (5.34). Within our approximation the right-hand side of equation (5.34) is small and describes the coupling between any two of the decoupled modes belonging to different boundaries. It is important only near mode crossings, where R_+ and R_- are given by:

$$R_+ = R_- = \frac{8-\sqrt{2}}{16\sqrt{2}-8}. \tag{5.35}$$

Equation (5.35) holds independently of the particular crossing.

Due to the logarithmic terms the eigenfrequencies of the decoupled modes belonging to the dispersion relation (5.34) have non-zero imaginary parts, i.e. all modes having $n_\pm \geqslant 1$ are damped. An approximation for their real parts is obtained by neglecting the logarithmic terms:

$$\mathscr{R}\bar{\sigma}_\pm \approx \pm\left(\frac{2\pi n_\pm}{kM}\right)^{1/2}. \tag{5.36}$$

A further consequence of the logarithmic terms is the existence of the two modes having $n_{\pm}=0$. However, contrary to the modes with $n_{\pm}\geqslant 1$ these two modes are unstable.

We could have obtained the decoupled modes also similarly to Section 5.3 by adopting the radiation condition (3.4) at one boundary and a suitable choice of the integration constants. If we replace the radiation condition (3.4) at one of the boundaries by the radiation condition (3.5) (equivalent to equation 5.28), we obtain as dispersion relation equation (5.32) or (5.33) with constant R_- or R_+, provided a critical layer occurs within the flow. (Otherwise no solution exists.) $R_-=R_+$ is found to be equal to $\sqrt{2}/4$ for outgoing radiation and equal to $\sqrt{2}/8$ for incoming radiation. Thus we also obtain in these cases essentially the decoupled modes discussed above but with an additional damping, which is slightly higher for incoming radiation.

We have plotted the eigenfrequencies of the two sets of decoupled modes belonging to the dispersion relation (5.34) for $k=1$ as a function of M in Fig. 7. The two modes, whose critical layer is closest to the boundary to which they belong to, are the unstable modes having $n_{\pm}=0$. The pattern speed of the damped modes having $n_{\pm}\geqslant 1$ is well represented by the approximation (5.36). Growth and damping rates decrease with increasing M and $n_{\pm}$.

The resonances of the decoupled modes may now be treated as in Section 5.2. Applying equation (5.16) to the mode crossings we find that at a mode crossing ε is real and positive and the derivatives of the dispersion relations are approximately given by

$$\frac{\partial D_{\pm}}{\partial \omega}\approx \pm 2\left(\frac{2\pi n_{\pm}}{kM}\right)^{1/2}. \tag{5.37}$$

Accordingly any of the mode crossings should give rise to a bubble of resonance instability. However, according to equation (5.16) the damping and growth rates of such bubbles of instability are shifted by the intrinsic growth or damping rates of the decoupled modes.

In Fig. 8 we have plotted the eigenfrequencies according to the dispersion relation (5.34) which contains the coupling of modes. A comparison with Fig. 7 shows that the decoupled modes are in fact a reasonable approximation to the full dispersion relation except near mode resonances. In accordance with our considerations above all crossings have unfolded into some kind of shifted instability bubble. However, since the decoupled modes are not neutral, exact mode crossings occur only at $\mathscr{R}\omega=0$ for $n_+=n_-$. Therefore the typical (shifted) instability bubble occurs only for these crossings and becomes less well pronounced as the critical layer of the mode crossing shifts towards the boundaries. Generally the resonance effect leads to an enhanced damping or growth of one of the crossing modes and to a decreased damping or growth of the second. In this sense the resonance bubble may be regarded as superimposed on the intrinsic growth or damping of the decoupled modes.

For completeness and comparison we have plotted in Fig. 9 the eigenfrequencies according to the exact dispersion relation which reads:

$$\bar{\sigma}_-^3\,\frac{[2\zeta_-+1-4\varkappa-2\zeta_-(1-4\varkappa/\zeta_-)^{1/2}]\;{}_1F_1(5/4-\varkappa,\,5/2,\,\zeta_-)+(4\varkappa+5)\;{}_1F_1(1/4-\varkappa,\,5/2,\,\zeta_-)}{[2\zeta_-+1-4\varkappa-2\zeta_-(1-4\varkappa/\zeta_-)^{1/2}]\;{}_1F_1(-1/4-\varkappa,\,-1/2,\,\zeta_-)+(4\varkappa-1)\;{}_1F_1(-5/4-\varkappa,\,-1/2,\,\zeta_-)}$$

$$-\bar{\sigma}_+^3\,\frac{[2\zeta_++1-4\varkappa+2\zeta_+(1-4\varkappa/\zeta_+)^{1/2}]\;{}_1F_1(5/4-\varkappa,\,5/2,\,\zeta_+)+(4\varkappa+5)\;{}_1F_1(1/4-\varkappa,\,5/2,\,\zeta_+)}{[2\zeta_++1-4\varkappa+2\zeta_+(1-4\varkappa/\zeta_+)^{1/2}]\;{}_1F_1(-1/4-\varkappa,\,-1/2,\,\zeta_+)+(4\varkappa-1)\;{}_1F_1(-5/4-\varkappa,\,-1/2,\,\zeta_+)}=0. \tag{5.38}$$

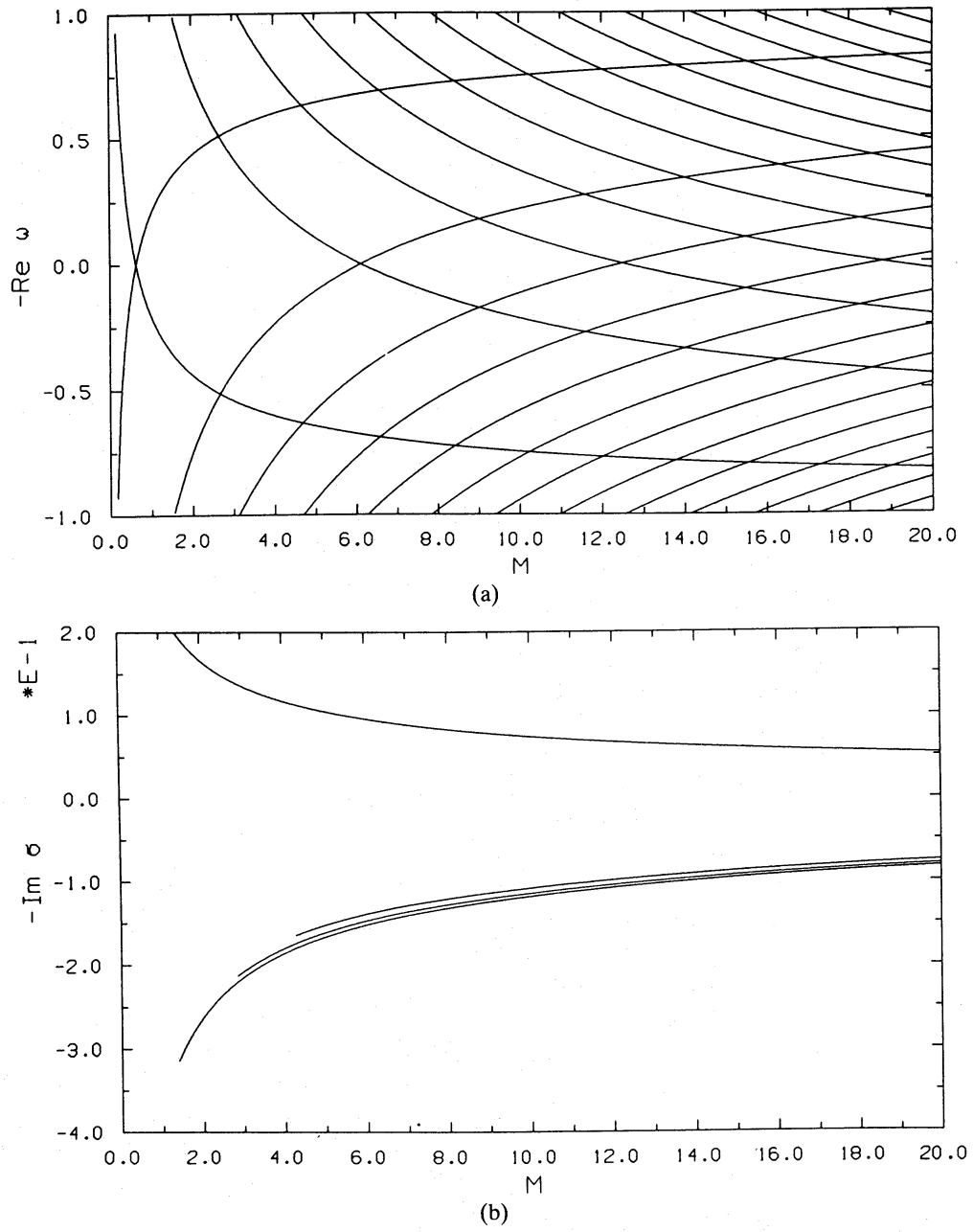

Figure 7. Pattern speeds $-\mathscr{R}\omega$ and growth or damping rates $-\mathscr{I}\sigma$ of the two sets of decoupled modes in the case of equal densities inside and outside the shear layer as a function of the Mach number M for wavenumber $k=1$. $-\mathscr{I}\sigma$ is plotted only for modes having $0\leqslant n_{\pm}\leqslant 3$.

Except for $n_{\pm}=0$ in the limit $M\rightarrow 0$ the dispersion relation (5.34) (Fig. 8) turns out to be an adequate approximation to the exact relation (5.38) (Fig. 9), which is not surprising, since the expansion used for the derivation of (5.34) is not valid for $M\rightarrow 0$. The two modes with $n_{\pm}=0$ unfold into a shifted band of instability at $\mathscr{R}\omega=0$ for $M\rightarrow 0$ only if $k<0.64$. For $k>0.64$ and $M\rightarrow 0$ they become neutral with a finite limit of $\mathscr{R}\omega$ in the range $0<|\mathscr{R}\omega|<1$ (see Fig. 9). A similar behaviour had also been found for the $n_{\pm}=0$ modes and the condition of zero Eulerian pressure perturbation at the boundaries (*cf.* Section 5.1). We shall comment on the limit $M\rightarrow 0$ in detail in Section 5.5.

Both in the approximation (Fig. 8) and for the exact model (Fig. 9) the correction of damping and growth rates due to mode coupling is weaker than the intrinsic damping or growth of the

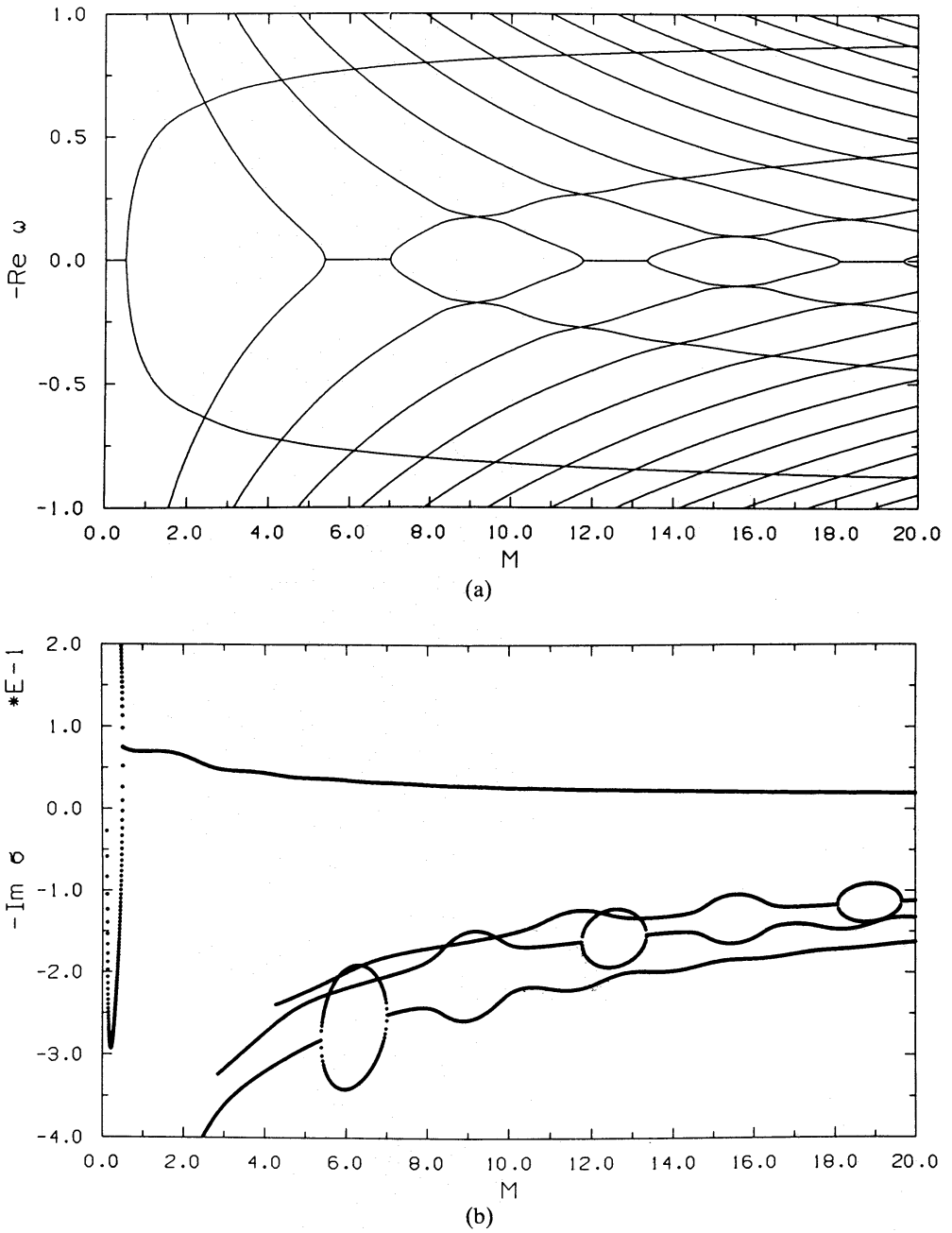

Figure 8. Pattern speeds $-\mathscr{R}\omega$ and growth or damping rates $-\mathscr{I}\sigma$ as a function of the Mach number M for wavenumber $k=1$ and equal densities inside and outside the shear layer according to the approximate dispersion relation (5.34). $-\mathscr{I}\sigma$ is plotted only for modes having $0\leqslant n_{\pm}\leqslant 3$.

decoupled modes, i.e. the stability properties are determined by the decoupled modes. This is mainly due to the zero density contrast between the regions inside and outside the shear layer. If the density contrast is increased, the damping and growth rates of the decoupled modes decrease and neutral modes are obtained in the limit of infinite density contrast (see equations 5.14 and 5.15).

Physically the increase of the density contrast means a reduction of acoustic radiation from the shear layer, i.e. the damping and growth of the decoupled modes for zero density contrast must be due to acoustic radiation. The same holds for modes which have no critical layer within the flow (*cf.* equations 5.31 and 5.26). However, not all modes react in the same way to energy loss by

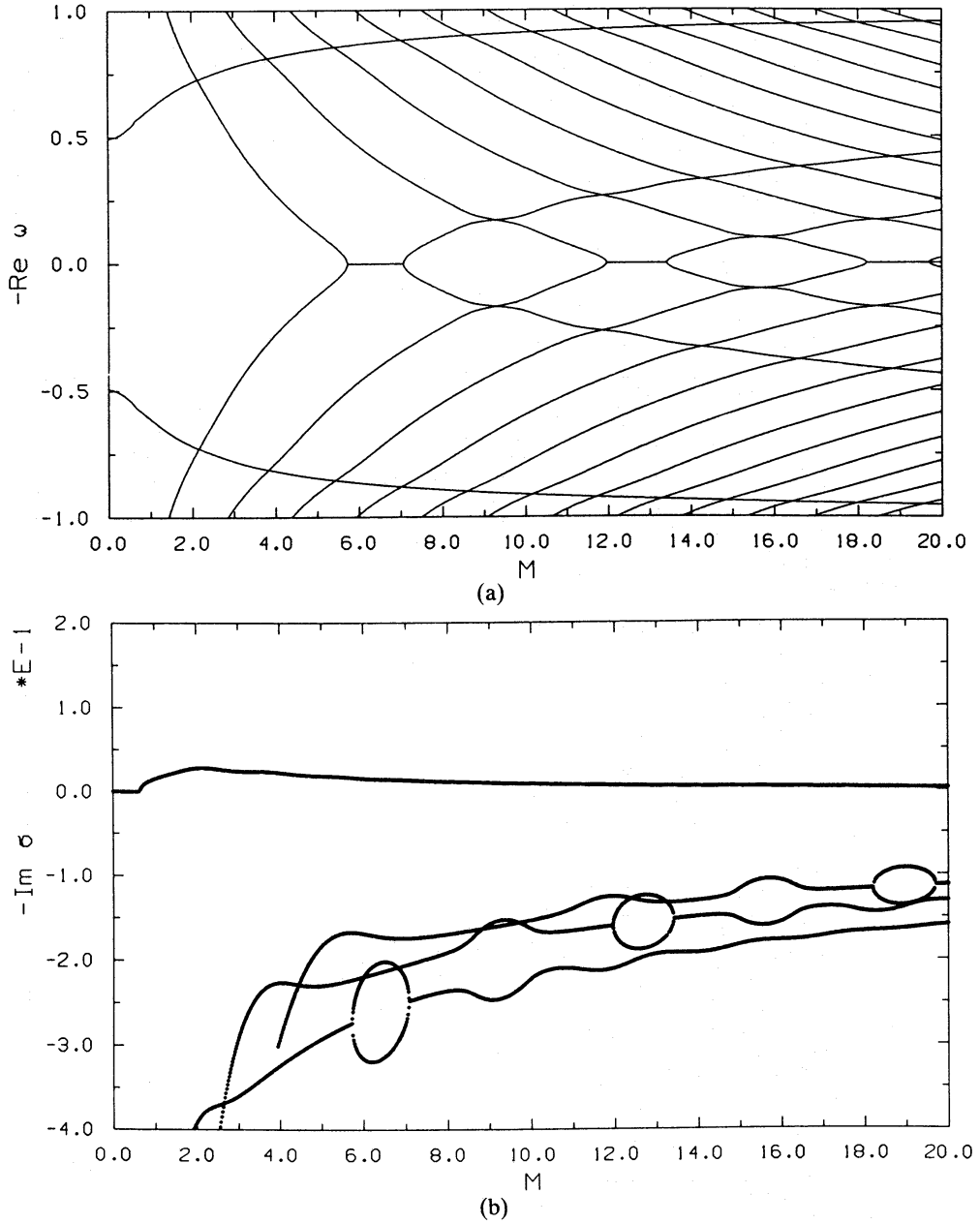

Figure 9. Same as Fig. 8 but according to the exact dispersion relation (5.38).

acoustic radiation. While all modes having $n_{\pm} \geqslant 1$ are damped, the modes with $n_{\pm} = 0$ become unstable, which might be taken as a hint on a different physical nature.

The pattern speeds of the decoupled modes having $n_{\pm} \geqslant 1$ are not much affected by a non-vanishing density contrast. If the density within the shear layer is smaller (bigger) than in the surrounding medium and the density contrast is increased the pattern speed changes from the value given by equation (5.36) to the value given by equations (5.14) and (5.15), where the lower (upper) sign has to be chosen. In other words, $2n_{\pm}$ changes to $2n_{\pm} \pm 1/2$ and the pattern speeds of modes corresponding to a radiation condition lie between the pattern speeds of the modes corresponding to the two extreme conditions of zero pressure and velocity perturbation. Again the modes with $n_{\pm} = 0$ behave in a different way. If the density contrast is increased and the density within the shear layer is bigger than outside, the pattern speeds of the modes change only slightly, whereas the modes entirely disappear in the opposite case.

Contrary to acoustic radiation, the effect of resonant interaction between different modes does not depend very much on the reflection properties of the boundaries (*cf.* Fig. 9). However, as the density contrast is increased and the intrinsic growth and damping rates of the decoupled modes are decreased, radiation is no longer the dominant effect and the stability properties given by the superposition of both effects are determined by resonant interactions rather than by the decoupled modes only. In the limit of an infinite density contrast we obtain pure resonance instabilities as discussed in Section 5.2 (see also Figs 3 and 6). These instabilities occur in bands rather than in a continuous fashion as stabilization or destabilization by radiation. The general intermediate case is a mixture of both kinds of instabilities occurring at the same time.

As in the case of perfectly reflecting boundaries the modes having no critical layer within the flow (equation 5.31) and the modes having a critical layer within the flow and $n_{\pm} \geqslant 1$ are continuously connected. However, to show this explicitly, the exact dispersion relation (5.38) has to be used, since the expansion (5.2)–(5.4) is not valid for small $|\zeta|$.

In the limit $k \to 0$ (vortex sheet approximation) all modes having $n_{\pm} \geqslant 1$ disappear (see equations 5.31 and 5.36). The behaviour of the modes having $n_{\pm} = 0$ follows from equation (5.38) for $\zeta_{\pm} \to 0$:

$$\omega^2 M^2 = 1 + M^2 \pm (1 + 4M^2)^{1/2}. \tag{5.39}$$

The lower sign in equation (5.39) corresponds to the modes with $n_{\pm} = 0$. They form an instability band for $M < \sqrt{2}$. Equation (5.39) is the dispersion relation for the compressible vortex sheet as given by Landau (1944) and discussed by Ray (1982) and Choudhury & Lovelace (1984). As the whole spectrum of modes having $n_{\pm} \geqslant 1$, which we shall identify with the sonic modes of the system in the next section, disappears for $k \to 0$, we conclude that results based on the vortex sheet approximation have to be interpreted with caution.

5.5 THE LIMIT OF LOW MACH NUMBERS

It has been shown in Section 5.1 that the general solution of the perturbation equation in the limit of zero Mach number can be expressed as the superposition of Bessel functions (*cf.* equation 5.8). This solution may be regarded as the first term of an expansion of the general solution in a power series in the Mach number M and we shall use it in the following to derive dispersion relations valid in the limit of low Mach numbers.

No solution is found, if we require the velocity perturbation to vanish at both of the boundaries (equation 3.3), i.e. the discrete spectrum is empty. This is in agreement with the results of Section 5.2, where no mode having a finite eigenfrequency for $M \to 0$ has been found for this boundary condition. The discrete spectrum is empty, since the limit $M \to 0$ corresponds to an incompressible fluid, which does not allow for internal waves except for waves which are supported by the gradient of vorticity, i.e. by its singularities at $z = \pm 1$. However, these waves are also excluded by the requirement of a zero velocity perturbation at $z = \pm 1$. We note that the limit $M \to 0$ with rigid boundary conditions is identical with the stability problem for the standard incompressible plane Couette flow, and it is well known that no discrete spectrum exists in this case (*cf.* Drazin & Reid 1981).

If we require the pressure perturbation to vanish at both of the boundaries we find two modes whose existence is due to the discontinuities of the velocity gradient at $z = \pm 1$. Their eigenfrequencies are given by:

$$k^2 \omega^2 = \frac{(1+k)^2 - (1-k)^2 \exp(4k)}{1 - \exp(4k)}. \tag{5.40}$$

For $k > 1.2$ they are neutrally stable with $0 < |\omega| < 1$ and for $k < 1.2$ their eigenfrequencies form a complex conjugate pair with $\mathscr{R}\omega = 0$. Comparing these modes with the modes described in

Section 5.2 having zero pressure perturbation at the boundaries we find exact agreement for $M=0$, if we identify them with the two modes having $n_{\pm}=0$.

Applying the radiation condition (3.4) instead of the condition $Q=0$ at both of the boundaries qualitatively the same result is obtained, where the dispersion relation is now given by:

$$k^2\omega^2=\tfrac{1}{4}[(1-2k)^2-\exp(-4k)]. \tag{5.41}$$

The eigenfrequencies described by equation (5.41) are neutrally stable for $k>0.64$ and form a complex conjugate pair for $k<0.64$. Again these modes can be identified with the corresponding ones described in Section 5.4 and having $n_{\pm}=0$.

Equation (5.41) is the standard dispersion relation for the Kelvin–Helmholtz modes of the flow considered here [see equation 23.7 of Drazin & Reid (1981)]. Therefore the modes having $n_{\pm}=0$ are the Kelvin–Helmholtz modes and the first instability band occurring for small wavenumbers at small Mach numbers, which is due to the crossing, i.e. the resonant interaction of the two modes with $n_{\pm}=0$, is the Kelvin–Helmholtz instability. Furthermore, they are identical with the unstable modes described by Ray (1982) and Choudhury & Lovelace (1984). Regarding their physical origin they cannot be addressed as sound waves.

In addition to the two Kelvin–Helmholtz modes an infinite number of modes exists, whose eigenfrequencies in the case of perfectly reflecting boundaries for $M\to 0$ are approximately given by equation (5.26). The divergence of these eigenfrequencies for $M\to 0$ is a consequence of our particular normalization. If we normalize the velocities by the sound velocity within the shear layer instead of by the flow velocity at the edges of the shear layer, the frequencies have to be multiplied by the Mach number M and the eigenfrequencies according to equation (5.26) have a finite limit for $M\to 0$ in this normalization.

The limit $M\to 0$ can be achieved either by keeping the flow velocity fixed and increasing the sound velocity or by keeping the sound velocity fixed and decreasing the flow velocity. In the first case normalization by the flow velocity is appropriate and the limit $M\to 0$ yields an incompressible flow, where only the Kelvin–Helmholtz modes can survive. In the second case normalization by the sound velocity is appropriate and the limit $M\to 0$ yields a compressible medium at rest excluding any Kelvin–Helmholtz-type modes. However, the compressibility together with reflecting boundaries now allows for a discrete spectrum of sound waves. Their dispersion relation for perfectly reflecting boundaries is given by (normalization by the sound velocity):

$$\omega^2=1+\frac{\pi^2}{4}\left(\frac{n}{k}\right)^2. \tag{5.42}$$

Equation (5.26) is valid for large values of n and in this limit the dispersion relations (5.42) and (5.26) become identical after correcting for the different normalizations. Therefore all modes described by equation (5.26) and, since they are continuously connected, also all modes with $n_{\pm}\geqslant 1$ may be addressed as sound waves.

Thus we have confirmed our suspicion that the modes with $n_{\pm}=0$ and $n_{\pm}\geqslant 1$ have different physical origin. The two modes having $n_{\pm}=0$ are Kelvin–Helmholtz modes and their existence is due to the velocity profile. The modes having $n_{\pm}\geqslant 1$ are sound waves and their existence is due to compressibility. For small flow velocities (low Mach numbers) their pattern speed is too high for a critical layer to exist within the flow. As the flow velocity is increased above the sound speed and the pattern speed of the mode becomes comparable to the flow speed the critical layers of these modes enter the flow. The shear then causes a distortion of the pattern speed and thereby mode crossings between modes originally travelling in the positive and negative x-direction, which unfold into bands of instabilities.

5.6 COMPLETENESS OF THE DISCRETE SPECTRUM

In the cases where a critical layer of the mode occurs within the flow we have considered in the preceding sections only modes which already exist in the limit $|\varkappa| \to 0$, i.e. modes corresponding to non-negative integers $n_{(\pm)}$. For finite values of $|\varkappa|$ the dispersion relations derived on the basis of asymptotic expansions for $|\zeta| \to \infty$ contain additional logarithmic terms (see equations 5.13 and 5.29) which allow for further solutions of the dispersion relations and give rise to additional modes. Due to the logarithmic term for any value of $n_{(\pm)}$ considered so far a second solution exists with $|\zeta_{(\pm)}|<1$. However, this solution may be an artefact, since the asymptotic expansion used to derive the dispersion relations is not valid for $|\zeta|<1$. Moreover, these solutions could not be confirmed using the exact dispersion relations. But a lack of numerical confirmation cannot serve as proof for the non-existence of these modes, in particular since they are expected to lie very dense and numerical difficulties may arise. Therefore their existence is not yet entirely excluded.

Modes corresponding to negative integers $n_{(\pm)}$ have been excluded in the limit $|\varkappa| \to 0$, since they have no critical layer within the flow. For finite $|\varkappa|$ the logarithmic term causes these modes to have a critical layer within the flow and for each $n_{(\pm)}$ having $2n_{(\pm)} \pm 1/2<0$ we get a pair of complex conjugate eigenfrequencies. The critical layer of the corresponding modes lies close to the boundaries $[|\mathscr{R}\bar{\sigma}_{(\pm)}| \approx (\sqrt{2}/2)(1/M)]$. For high wavenumbers and small $|n_{(\pm)}|$ the imaginary part of the complex conjugate pair has a maximum as a function of $|\varkappa|$ and decreases again for high $|\varkappa|$ thus forming a pair of neutral modes above some critical value of $|\varkappa|$. One of these modes has $|\bar{\sigma}_{(\pm)}|<(\sqrt{2}/2)(1/M)$ and can also exist in a subsonic flow, the other has $|\bar{\sigma}_{(\pm)}|>(\sqrt{2}/2)(1/M)$ and lies always in the supersonic regime. Since the derivative of the dispersion function changes sign at $|\bar{\sigma}_{(\pm)}|=(\sqrt{2}/2)(1/M)$ (see equation 5.19), these modes show opposite behaviour at a mode crossing. Crossings of modes of the same type belonging to different boundaries will unfold into bands of instabilities, whereas crossings of modes of different type yield avoided crossings. If these additional modes having $2n_{(\pm)} \pm 1/2<0$ are not an artefact of the asymptotic expansion used, we expect additional instabilities even in the subsonic regime. Therefore the numerical confirmation of their existence by using the exact dispersion relations is necessary and important.

We have found a type of mode satisfying the exact dispersion relations, whose eigenfrequencies have the same behaviour and are very close to the additional eigenfrequencies described. They satisfy the boundary conditions and the perturbation equation except at the critical layer. At the critical layer either the velocity or the pressure perturbation has a discontinuity. Therefore these modes have to be excluded and it is likely that the additional modes predicted above are an artefact of the asymptotic expansion. However, a numerical analysis cannot prove the non-existence of modes. Since the modes found are physically admissible except at the critical layer, we speculate that they may become admissible, if the physical conditions at the critical layer are changed, e.g. by a non-zero vorticity gradient. Possibly they are the modes introduced and supported by a vorticity gradient, which cannot exist here, since the vorticity gradient vanishes in our model.

Apart from introducing additional possibly unstable modes a vorticity gradient has influence on the growth rates. For rotating shear flows it usually leads to an additional damping (Glatzel 1987a), but as shown by Papaloizou & Pringle (1987) it may also destabilize the flow, if the gradient of the ratio of vorticity to density is positive at corotation.

6 A physical mechanism for the instabilities

We have shown in a previous paper (Glatzel 1987b) how a pseudo-energy may be defined for a neutral mode in a rotating shear layer having constant sound speed and constant angular

momentum distribution. [For the definition of the energy of sound waves in shear flows see also Möhring (1973) and Friedman & Schutz (1978a, b).] This pseudo-energy was used to derive a physical picture of the instability. Since the stability problems for the rotating and the linear shear layer considered here are apart from obvious modifications identical (*cf.* Section 4), we can immediately apply the results of Glatzel (1987b) concerning the physical mechanism for the instabilities to the linear shear layer. The analysis given there corresponds to the limit $|\varkappa| \to 0$ and we shall for simplicity restrict ourselves to this limit here too, since the general case is qualitatively identical. It is obvious how to transfer the derivations for the rotating shear layer to the linear shear layer and we shall omit them here.

We consider a neutrally stable mode obtained by the requirement of zero pressure or velocity perturbation at one boundary and an appropriate choice of the integration constants. The energy flux dE/dt needed to increase the amplitude of this mode by an external driving force exerted at the perfectly reflecting boundary is proportional to

$$\frac{dE}{dt} \sim -\bar{\sigma} n_z. \tag{6.1}$$

$n_z = \pm 1$ denotes the vertical component of the normal vector of the perfectly reflecting boundary, at whose position $\bar{\sigma}$ in equation (6.1) has to be evaluated.

For $(dE/dt)<0$ the energy of the system decreases as the amplitude of the mode grows. Consequently the mode has negative energy. Conversely, if $(dE/dt)>0$, the mode has positive energy. Therefore the sign of dE/dt as given by equation (6.1) may be identified with the sign of an energy-like quantity associated with the mode, called pseudo-energy in the following. If the reflecting boundary lies at $z=+1$ and the mode has a critical layer within the flow, we have $n_z=+1$ and $\bar{\sigma}>0$ and the pseudo-energy of the mode is negative. It is also negative if the reflecting boundary lies at $z=-1$. If a mode having negative energy loses energy due to acoustic radiation, it becomes unstable and its amplitude increases, whereas energy supply stabilizes the mode. The negative pseudo-energy then also provides the physical explanation for the situation found in Section 5.3, where the neutral modes corresponded to zero energy flux and turned into growing modes for energy loss and into damped modes for energy supply.

Also the resonance instabilities discussed in Section 5.2 may be interpreted using the pseudo-energy. In this case we have to compare the energy of two modes. However, for a comparison to be meaningful the same conditions have to be used for both of the modes, i.e. the same sign of n_z has to be taken. Accordingly, the pseudo-energy of neutral modes belonging to different boundaries and having a critical layer within the flow has opposite sign. In this sense the sign of the pseudo-energy is related to the sign of the derivative of the dispersion relation of the decoupled modes (see Section 5.2) which determines the stability properties at a mode crossing. If two modes interact, whose pseudo-energy has opposite sign, the amplitude of both of them can grow by an exchange of energy, even if the total energy of the system is to be conserved. The result is a band of instability. A similar interpretation of the stability properties in terms of the pseudo-energy for the case of partially reflecting boundaries seems possible too, although we have not calculated the corresponding neutral modes and their pseudo-energy explicitly.

7 Conclusion

The stability of a simple supersonic shear layer has been re-examined using analytical methods. In particular, the solution of the perturbation equation has been given in analytical form. Contrary to previous investigations we found that a density contrast between the shear layer and the surrounding medium, i.e. different boundary conditions for the perturbed quantities have a strong influence on the stability properties of the shear layer. Not only the magnitude of the

growth rates of the instabilities changes by a substantial amount, but also the appearance of the unstable modes is entirely different with and without density contrast. This is due to different physical mechanisms being dominant in the two cases. Accordingly, in the applications, e.g. in galactic and extragalactic jets, where density gradients in shear layers are likely to occur, the qualititative change of the stability properties due to density contrasts cannot be ignored.

Three extreme cases have been discussed in detail: if the densities inside and outside the shear layer are equal and if the density inside the shear layer is much lower or higher than in the surrounding medium. In each of these cases a twofold infinite set of sonic modes exists which is associated with the two edges of the shear layer. In the limit of low Mach numbers, i.e. for a compressible medium at rest confined by two parallel reflecting planes these two sets are the sound waves travelling parallel to the boundaries in the positive and negative direction respectively. As a linear shear flow is introduced in this configuration and its velocity is increased the pattern speed of the sound waves becomes comparable to the flow speed above a certain Mach number in the supersonic regime. They get a critical layer within the flow and due to the shear their pattern speed becomes distorted and follows the speed of the edge of the shear layer moving originally in the opposite direction. Thus the effect of the shearing motion produces crossings of the pattern speed, i.e. resonances between the two sets of sound waves.

It is particularly obvious for a medium at rest, i.e. the limit of low Mach numbers, that at least some reflection is necessary for the existence of a discrete spectrum. For a high density contrast between the shear layer and the surrounding medium the reflection is perfect but for the case of equal densities inside and outside the shear layer the origin of reflection is less obvious. Here the reflection of sound waves which guarantees the existence of a discrete spectrum is provided by the velocity profile itself, i.e. by the discontinuity of the velocity gradient at the edges of the shear layer.

Due to the same physical origin the number and the qualitative behaviour of the pattern speed of these sonic modes is essentially independent of the density contrast between the shear layer and the surrounding medium. Only a small shift in the pattern speeds is found, if the ratio of the densities is varied from zero to infinity.

In addition to the sonic modes two Kelvin–Helmholtz-type modes exist associated again with the two edges of the shear layer, which owe their existence to the velocity profile, i.e. its discontinuities at the edges of the layer. If the density in the surrounding medium is much larger than in the shear layer, the existence of these modes is excluded. The Kelvin–Helmholtz modes always have critical layers within the flow, even in the subsonic regime.

By replacing one of the perfectly reflecting boundary conditions at one of the edges of the shear layer by a non-reflecting condition the two sets of modes belonging to different boundaries can be decoupled. If the non-reflecting condition corresponds to zero energy flux, neutrally stable modes are obtained, whereas outgoing waves yield growing and incoming waves damped modes. The stability properties of the case with two perfectly reflecting boundaries can now be understood as a superposition of the neutral modes belonging to the two boundaries, where all mode crossings have unfolded into bands of instabilities. It has been shown that the relative sign of the energy of modes belonging to different boundaries differs. Therefore by an exchange of energy the amplitude of both of the crossing modes can grow, even if the total energy of the system is conserved. Destabilization or damping by energy loss or energy supply due to acoustic radiation can be understood in a similar way by the existence of modes having negative energy.

For perfectly reflecting boundaries we find pure resonance instabilities, whereas the general case is determined both by resonances and radiation effects. In the case of zero density contrast radiation is dominant, the sonic modes have positive energy and are damped by acoustic radiation, whereas the Kelvin–Helmholtz modes have negative energy and are destabilized. The superimposed resonances do not change the stability characteristics here.

Considering the whole range of wavenumbers the sonic modes provide instabilities for any Mach number in the supersonic regime either by resonances or by radiation losses depending on the boundary condition. As it is difficult to avoid both types of instability at the same time, we conclude that most of the supersonic shear flows are unstable, even if rotation is included (*cf.* Glatzel 1987b) which might be relevant also for protostellar rings and the process of fragmentation (*cf.* Hawley 1987 and Goodman, Narayan & Goldreich 1987).

Since the pattern speed of the sonic modes in the medium at rest is supersonic, mode crossings and resonance instabilities for these modes can only occur in a supersonic shear flow. If the fluid at rest would allow for a discrete spectrum of other types of modes, in particular with lower pattern speeds, e.g. Alfvén waves or *g*-modes, the shear might produce resonance instabilities in the same way as for the sound waves even in the subsonic regime. In other words, we speculate that resonance instabilities and mode crossings will occur in a shear flow if there is a discrete spectrum of modes. The shear causes opposite distortion of the pattern speed of modes corresponding to waves travelling in opposite directions, which leads to mode crossings, if the shear velocity is of the order of the pattern speed of the modes in the fluid at rest. In this sense the stability of plane Couette flow in the subsonic regime is simply due to the non-existence of discrete modes having a suitable pattern speed. Also a change in the velocity profile (a non-zero vorticity gradient) might introduce additional low-frequency modes, which could give rise to resonance instabilities. Possibly these modes are responsible for the difference between the linear and the sinusoidal velocity profile treated by Choudhury & Lovelace (1984).

Apart from obvious modifications the stability problem of a rotating shear layer discussed in a previous paper (Glatzel 1987b) in connection with the instability of accretion tori found by Papaloizou & Pringle (1984) has been shown to be equivalent to the stability problem of the linear shear layer discussed here. Accordingly, the effect of rotation is not essential for the type of instability found by Papaloizou & Pringle (1984). Instead it may be regarded as an instability caused by the shear motion, which operates due to the particular model through sound waves, surface waves (Blaes & Glatzel 1986) and Kelvin–Helmholtz-type modes. If the model allows for magnetic fields or entropy gradients, Alfvén waves or *g*-modes possibly lead to instabilities in the same way as the modes discussed here. For differentially rotating stars this might be relevant for the determination of stable rotation laws or as an excitation mechanism of *g*-modes by the shear motion.

In a recent paper Narayan, Goldreich & Goodman (1987) considered the stability of a rotating shearing sheet. This configuration is essentially the same as the rotating cylinder discussed by Glatzel (1987b) and according to Section 4 there is also a close relation to the linear shear layer studied here. Consequently numerical results for identical boundary conditions do not differ. However, the approach and the physical interpretation of the results as well as some conclusions are different. In particular, for the case of perfectly reflecting boundaries unstable modes are not scattered randomly with no obvious pattern of occurrence. Rather they occur in the way described here exactly at the position of mode crossings of the decoupled modes. Furthermore, if feedback at the boundaries was essential in generating an instability, we expect reduced reflection at the boundaries to have a damping effect on the resonance instability bands. However, as long as the existence of the modes is not affected, the resonance instability is essentially independent of the reflection of sound waves at the boundaries (see Section 5.4 and Fig. 9).

Acknowledgments

I am grateful to Dr J. Pringle for comments and to Dr W. Möhring for bringing the papers by Goldstein & Rice (1973) and Koutsoyannis *et al.* (1980) to my attention.

References

Abramowitz, M. & Stegun, I., 1970. *Handbook of Mathematical Functions,* Dover Publications, New York.
Blaes, O. M., 1985. *Mon. Not. R. astr. Soc.,* **216,** 553.
Blaes, O. M. & Glatzel, W., 1986. *Mon. Not. R. astr. Soc.,* **220,** 253.
Blumen, W., Drazin, P. G. & Billings, D. F., 1975. *J. Fluid Mech.,* **71,** 305.
Cairns, R. A., 1979. *J. Fluid Mech.,* **92,** 1.
Choudhury, S. R. & Lovelace, R. V. E., 1984. *Astrophys. J.,* **283,** 331.
Craik, A. D. D., 1985. *Wave Interactions and Fluid Flows,* Cambridge University Press.
Drazin, P. G. & Reid, W. H., 1981. *Hydrodynamic Stability,* Cambridge University Press.
Drury, L. O'C., 1985. *Mon. Not. R. astr. Soc.,* **217,** 821.
Ferrari, A. & Trussoni, E., 1983. *Mon. Not. R. astr. Soc.,* **205,** 515.
Ferrari, A., Massaglia, S. & Trussoni, E., 1982. *Mon. Not. R. astr. Soc.,* **198,** 1065.
Friedman, J. L. & Schutz, B. F., 1978a. *Astrophys. J.,* **221,** 937.
Friedman, J. L. & Schutz, B. F., 1978b. *Astrophys. J.,* **222,** 281.
Glatzel, W., 1987a. *Mon. Not. R. astr. Soc.,* **225,** 227.
Glatzel, W., 1987b. *Mon. Not. R. astr. Soc.,* **228,** 77.
Goldreich, P. & Narayan, R., 1985. *Mon. Not. R. astr. Soc.,* **213,** 7P.
Goldreich, P., Goodman, J. & Narayan, R., 1986. *Mon. Not. R. astr. Soc.,* **221,** 339.
Goldstein, M. & Rice, E., 1973. *J. Sound Vibr.,* **30,** 79.
Goodman, J., Narayan, R. & Goldreich, P., 1987. *Mon. Not. R. astr. Soc.,* **225,** 695.
Hanawa, T., 1986. *Mon. Not. R. astr. Soc.,* **223,** 859.
Hardee, P. E., 1979. *Astrophys. J.,* **234,** 47.
Hawley, J. F., 1987. *Mon. Not. R. astr. Soc.,* **225,** 677.
Koutsoyannis, S. P., Karamcheti, K. & Galant, D. C., 1980. *AIAA J.,* **18,** 1446.
Landau, L., 1944. *Akad. Nauk. SSSR, Comptes Rendus (Doklady),* **44,** 139.
Luke, Y. L., 1969. *The Special Functions and Their Approximations,* Vol. 1, Academic Press, New York.
Luke, Y. L., 1977. *Algorithms for the Computation of Mathematical Functions,* Academic Press, New York.
Möhring, W., 1973. *J. Sound Vibr.,* **29,** 93.
Narayan, R., Goldreich, P. & Goodman, J., 1987. *Mon. Not. R. astr. Soc.,* **228,** 1.
Papaloizou, J. C. B. & Pringle, J. E., 1984. *Mon. Not. R. astr. Soc.,* **208,** 721.
Papaloizou, J. C. B. & Pringle, J. E., 1985. *Mon. Not. R. astr. Soc.,* **213,** 799.
Papaloizou, J. C. B. & Pringle, J. E., 1987. *Mon. Not. R. astr. Soc.,* **225,** 267.
Ray, T. P., 1982. *Mon. Not. R. astr. Soc.,* **198,** 617.